SAR Marine Applications

Currents and Objects

Martin Gade
Uni Hamburg, Institut für Meereskunde
martin.gade@uni-hamburg.de

Universität Hamburg
DER FORSCHUNG | DER LEHRE | DER BILDUNG

FAKULTÄT
FÜR MATHEMATIK, INFORMATIK
UND NATURWISSENSCHAFTEN

SAR Maritime Applications

Friday, 9 Sep, Morning:

1 - History & Basics
- Introduction
- Radar/SAR History
- Basics
- Scatterometer

2 - Wind and Waves
- SAR Wind Fields
- Storms, Tropical Cyclones
- Ocean Surface Waves
- Oceanic Internal Waves
- Marine Surface Films
- Rain

Friday, 9 Sep, Afternoon:

3 - Currents and Objects
- Surface Currents
- Sea Bottom Topography
- Ship Detection
- Oil Pollution Monitoring
- Sea Ice

4 - Practicals
- Sentinel 1 Toolbox:
- Georeferencing, Mosaics
- Image Interpretation
- Wind Fields, Oil Pollution,
- Sea Ice, Objects

Surface Currents

SAR Imaging of Surface Currents

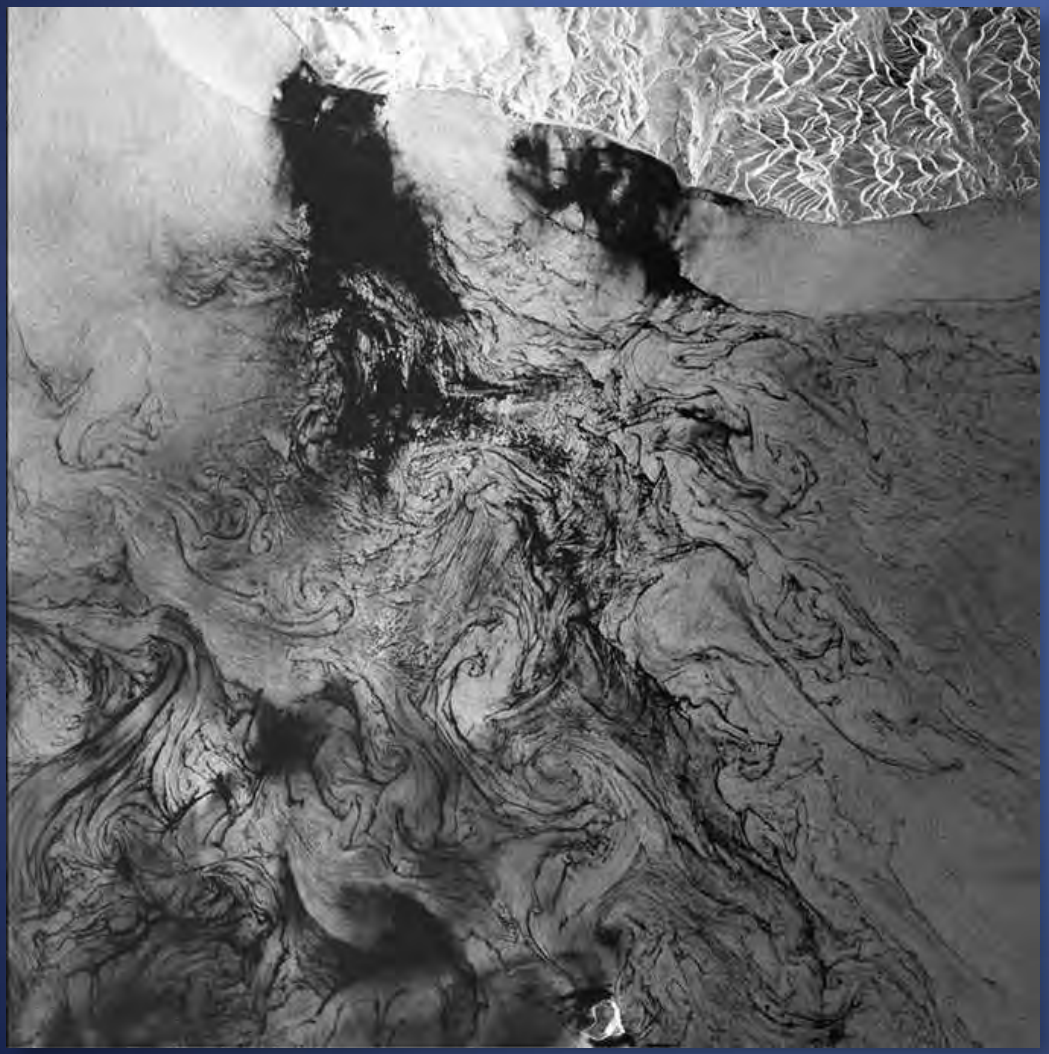

Slicks & eddies

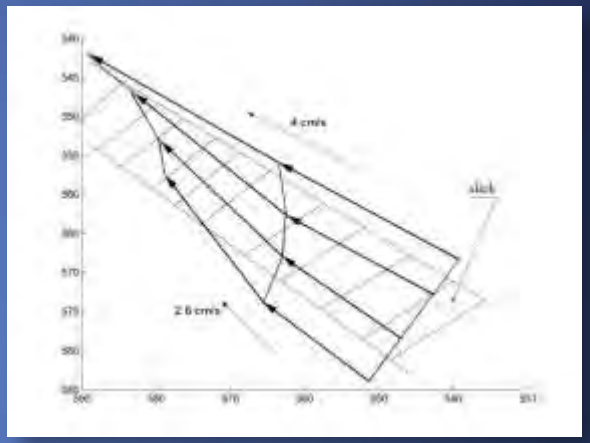

[Gade et al., 1998]

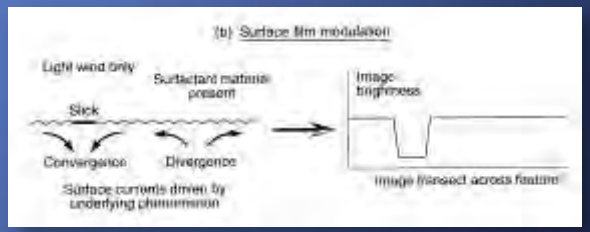

[Robinson, 2003]

ERS SAR Image (C-VV; 70 km × 70 km)
Bering Strait
(24 June 1997, 22:30 UTC, © ESA)

Hydrodynamic Processes at the Sea Surface

Imaging by SAR

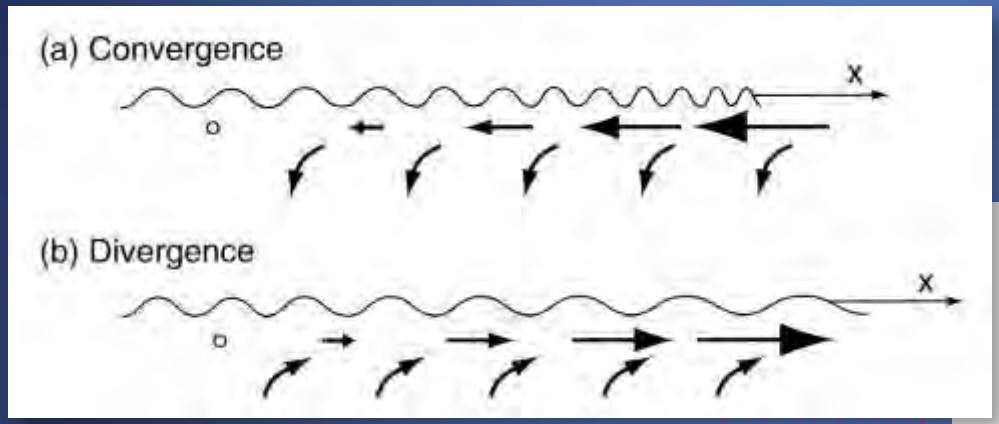

[Robinson, 2003]

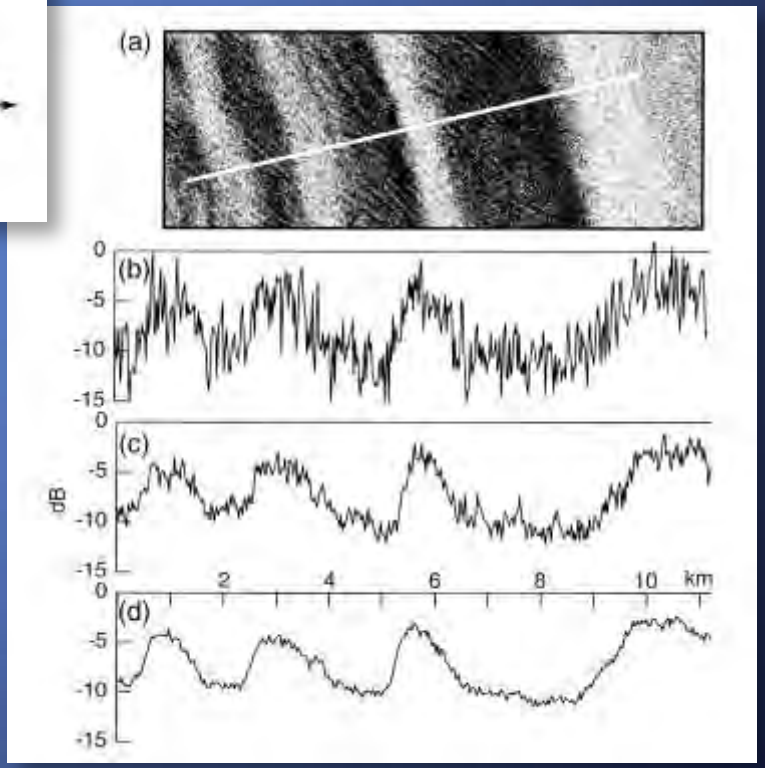

Along-Track Interferometric (ATI) SAR

TerraSAR-X / TanDEM-X

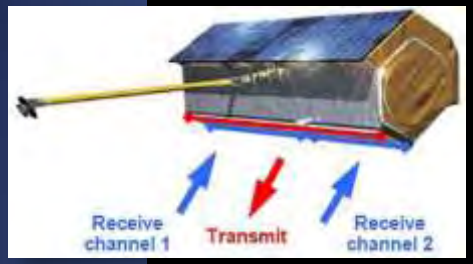

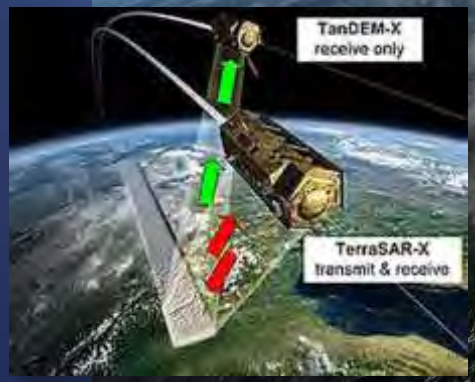

Along-Track Interferometric (ATI) SAR

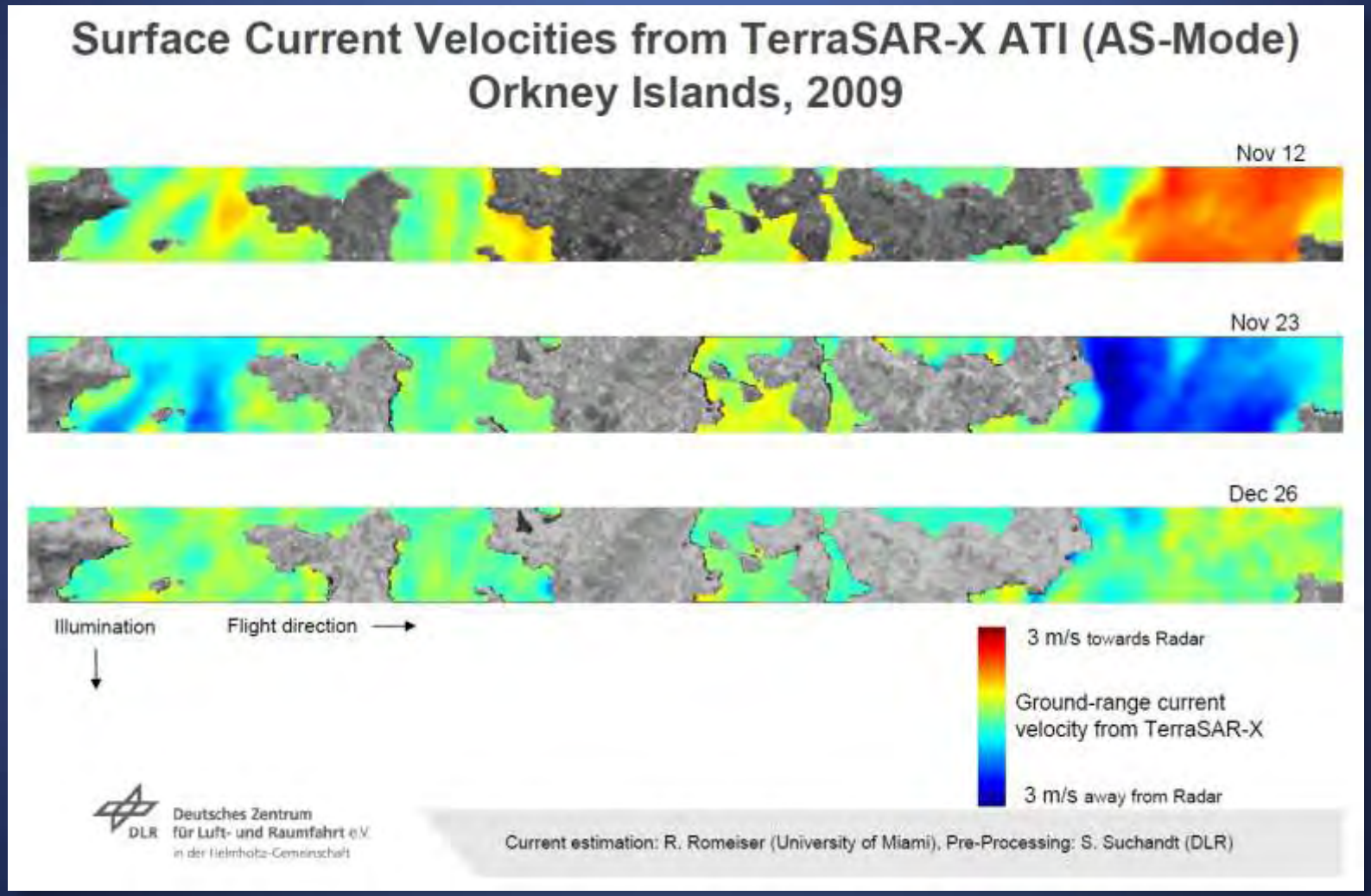

Along-Track Interferometric (ATI) SAR

TanDEM-X SAR Image (X-VV; 30 km × 30 km) Pentland Firth (Scotland) (26 February 2012, 06:41 UTC, © DLR)

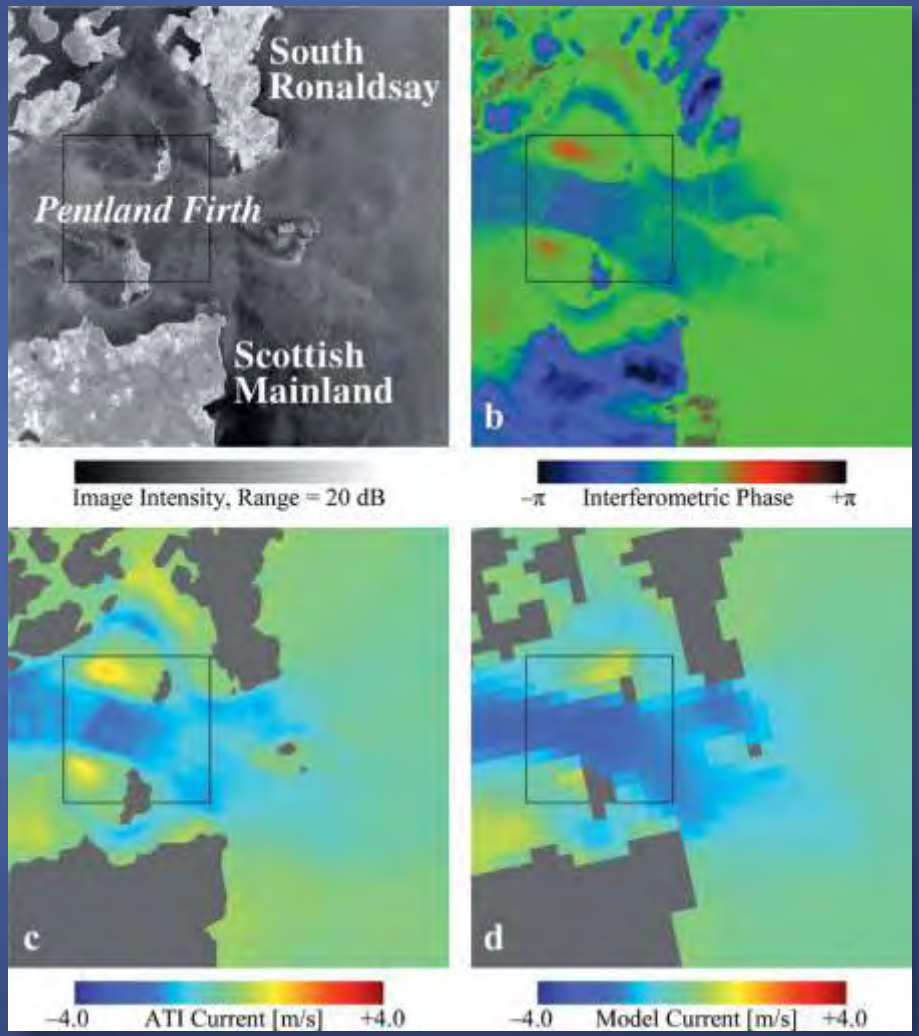

Interferometric phase image

radar look direction

Derived line-of-sight current field

Reference current field from numerical tide computation system

[Romeiser, 2013]

Along-Track Interferometric (ATI) SAR

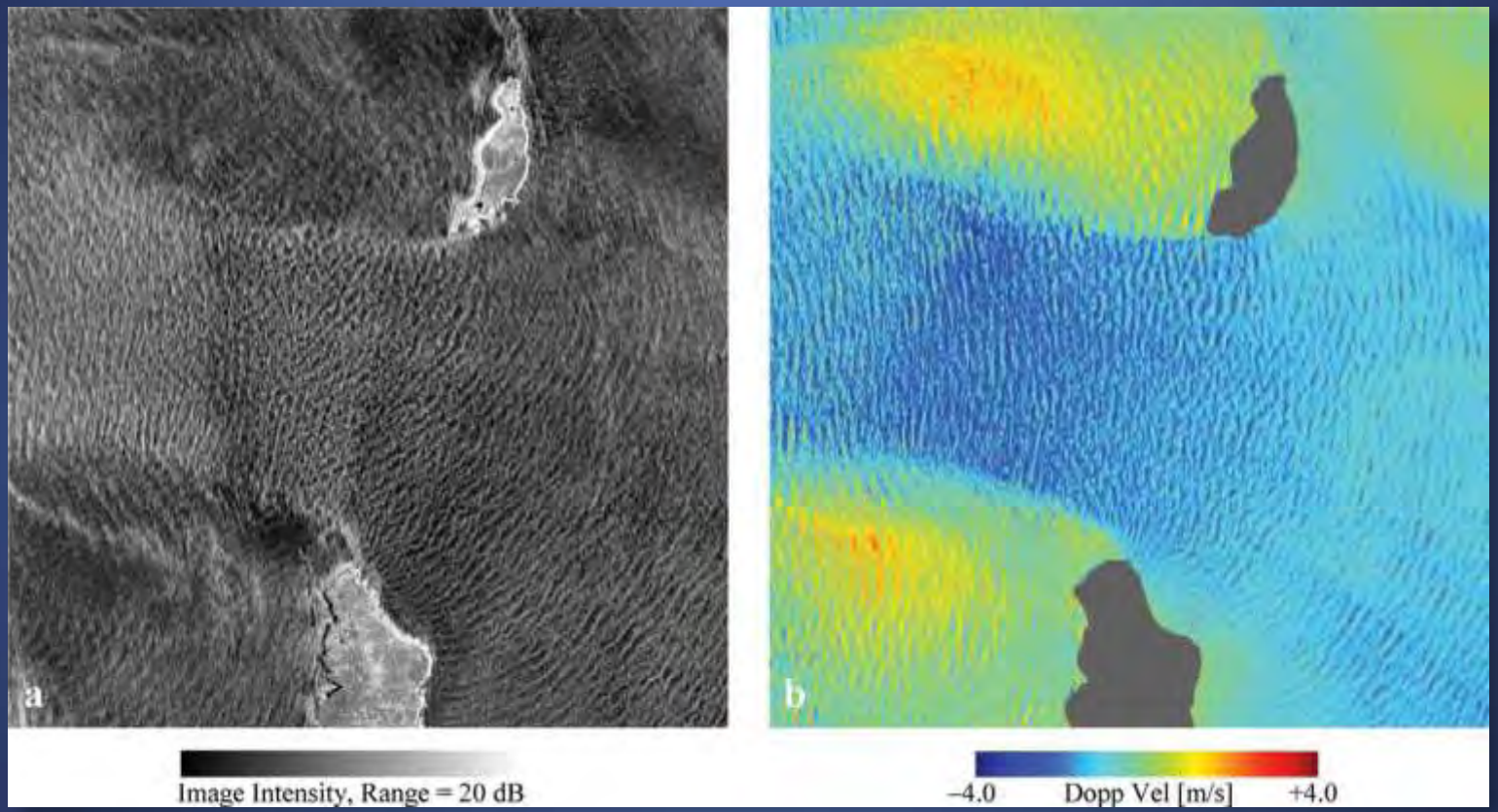

TanDEM-X SAR Image (X-VV; 10 km × 10 km)
Pentland Firth (Scotland)
(26 February 2012, 06:41 UTC, © DLR)

Derived line-of-sight current field:
full-resolution Doppler velocity image

radar look direction

[Romeiser, 2013]

Along-Track Interferometric (ATI) SAR

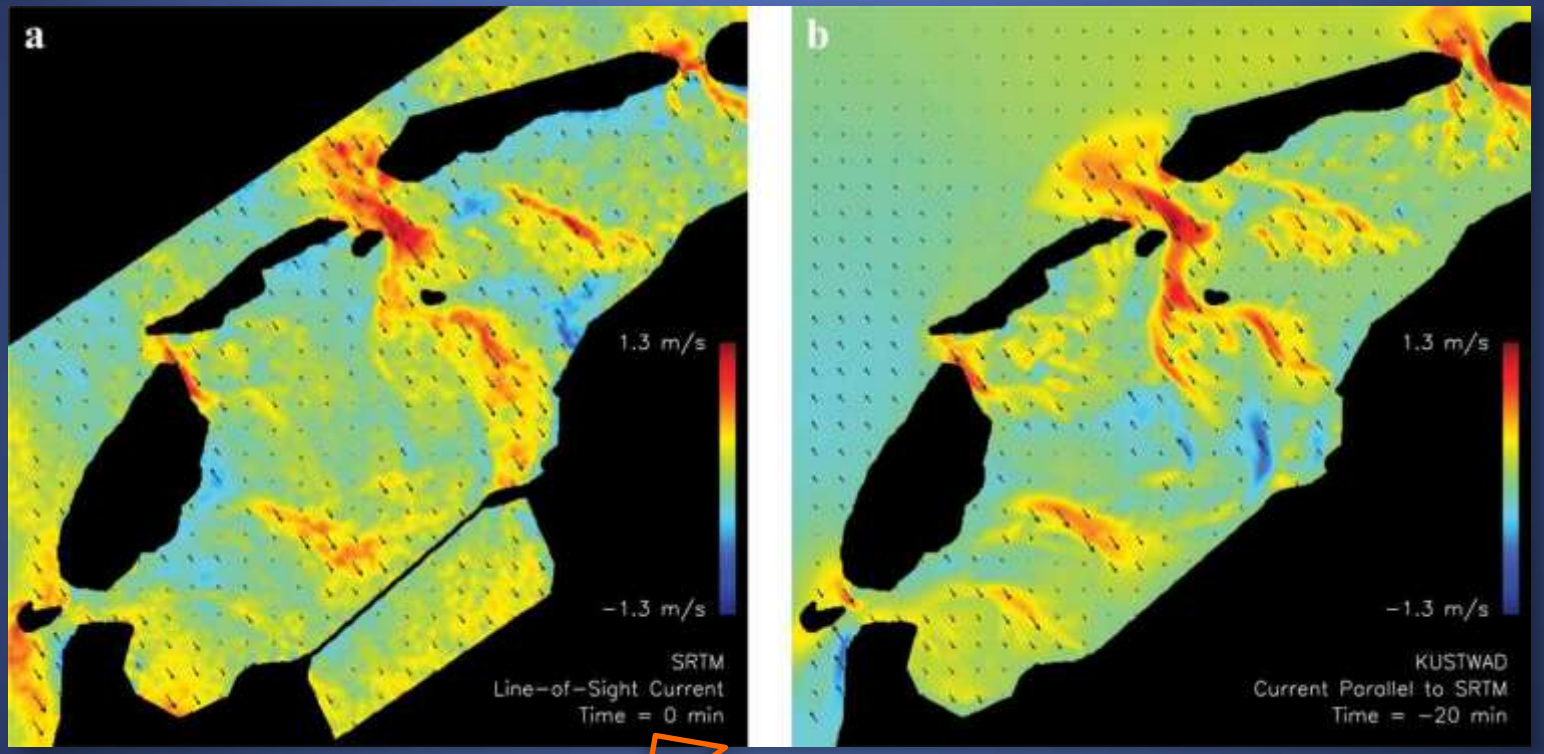

SRTM (X-VV; 70 km × 70 km)
Dutch Wadden Sea
(15 February 2000, 12:34 UTC)

Reference current field from a numerical circulation model

[Romeiser, 2013]

Along-Track Interferometric (ATI) SAR

SRTM (X-VV; 55 km × 30 km) Elbe river

Current field from a numerical model

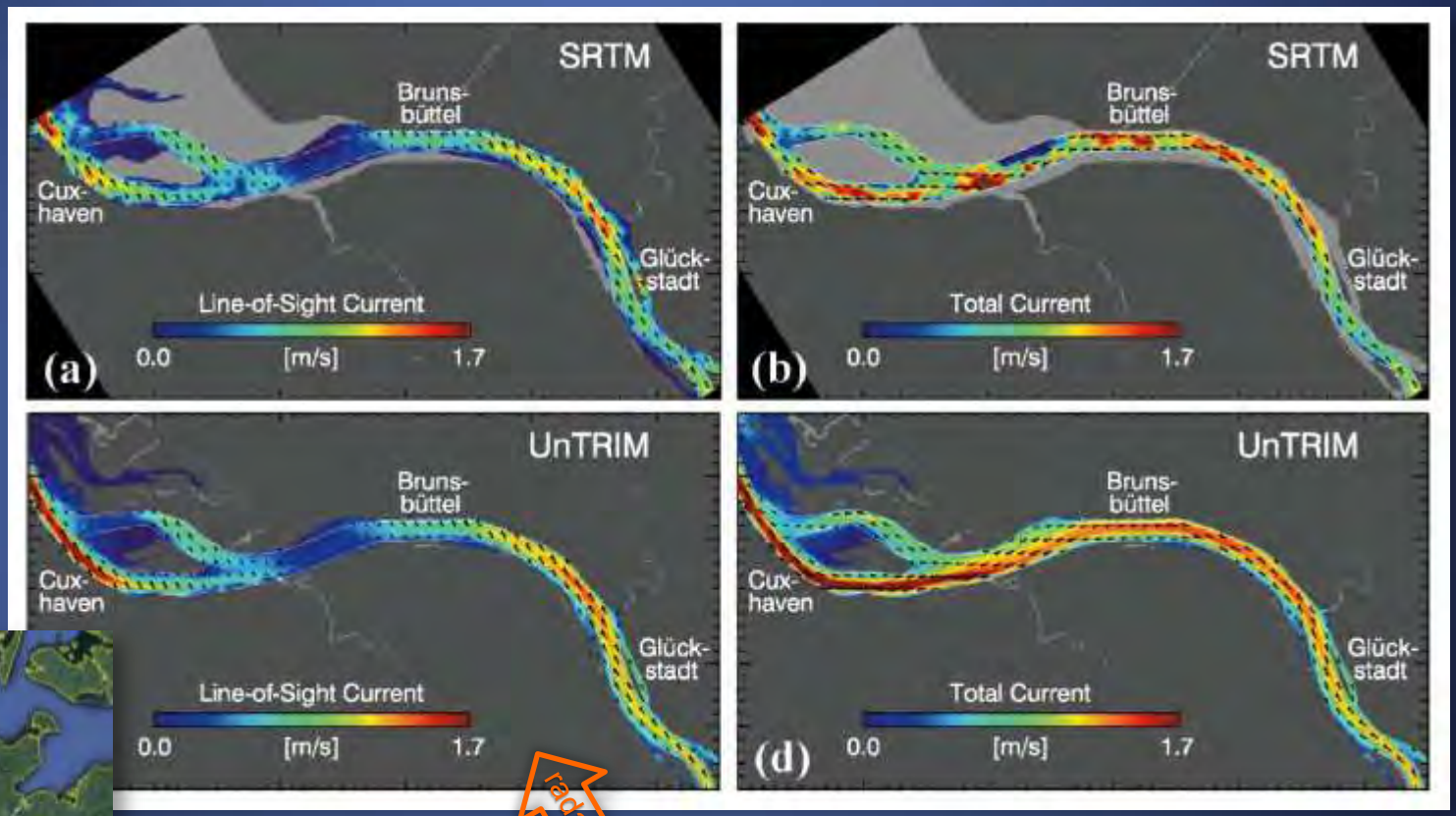

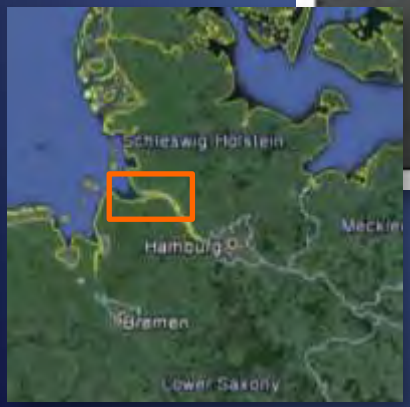

[Barale & Gade, 2008]

Radial Doppler Velocities from SAR Imagery

Mean radial Doppler velocities derived from 4 years (‘07-‘11) ASAR data

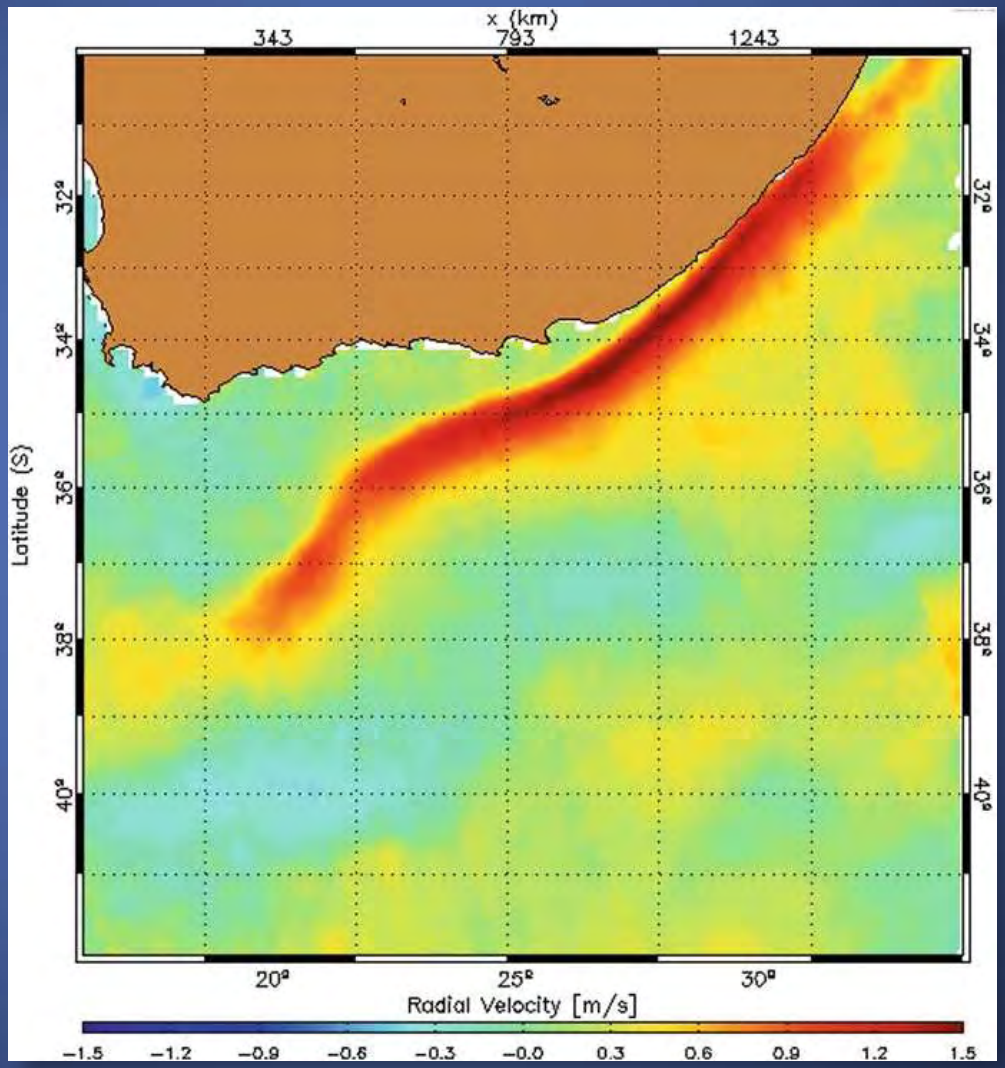

Mean westward current; Agulhas Current (S Africa)

[Barale & Gade, 2014]

Surface Currents
Take-Home Messages

Derivation of sea-surface currents:

- tracking of features
- Along-Track Interferometry
- Doppler velocities

Sea Bottom Topography

SAR Imaging of Sea Bottom Topography

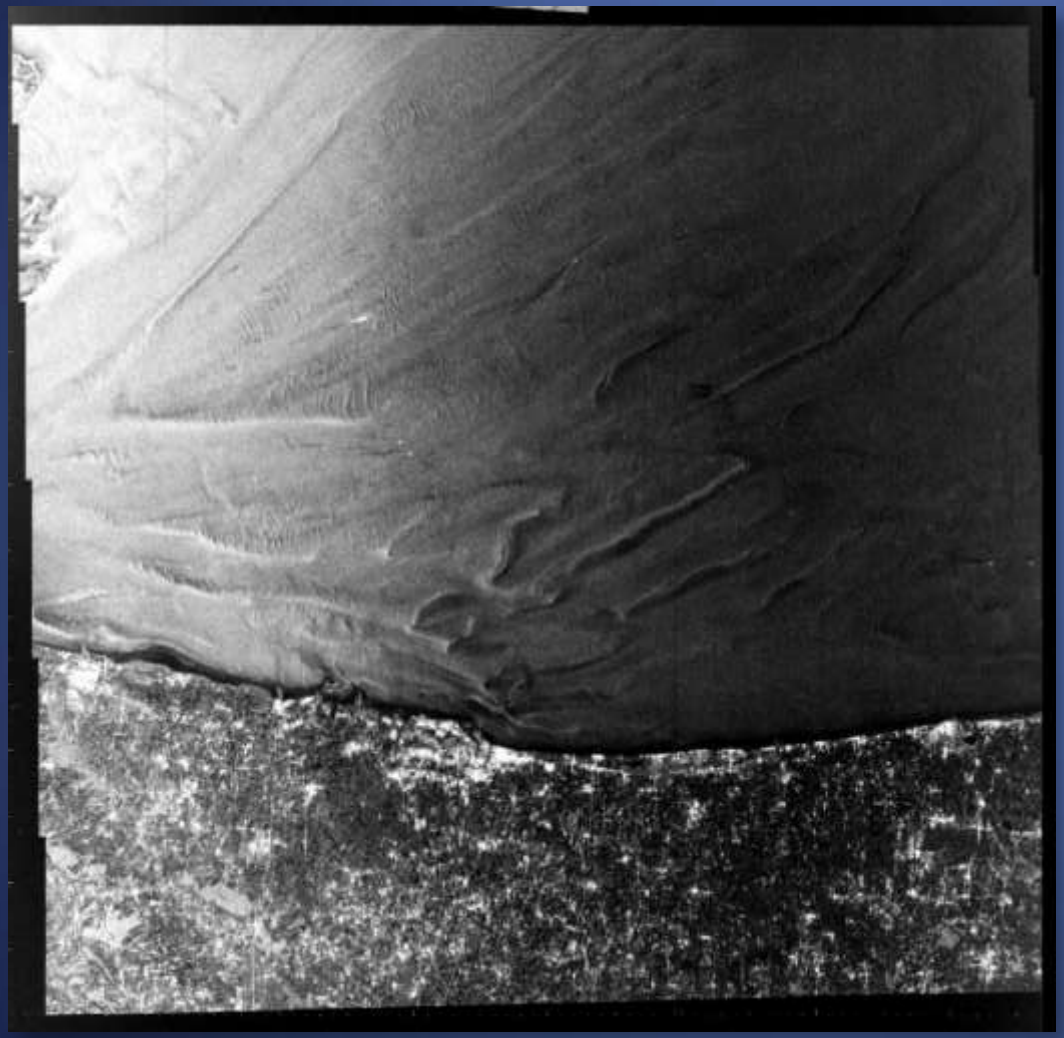

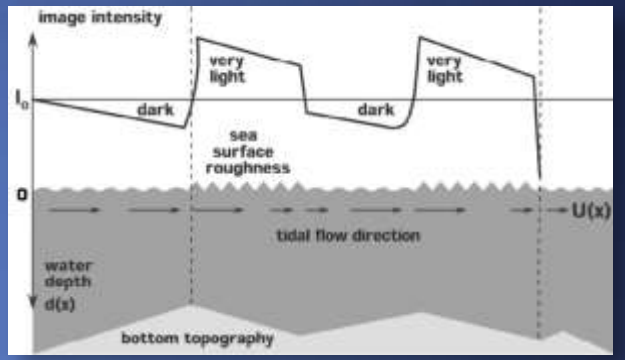

[Jackson & Apel, 2004]

Seasat SAR Image (L-HH, 100 km × 100 km)
English Channel
(August 1978, © NASA)

SAR Imaging of Sea Bottom Topography

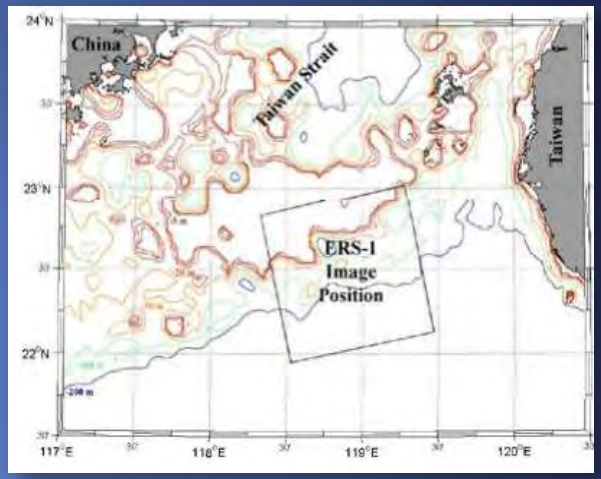

[Jackson & Apel, 2004]

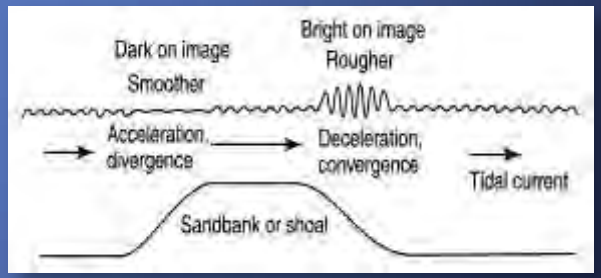

[Robinson, 2003]

ERS-1 SAR Image (C-VV, 100 km × 100 km)
Taiwan Tan Shoals
(27 July 1994, 14:31 UTC, © ESA)

SAR Imaging of Sea Bottom Topography

[Jackson & Apel, 2004]

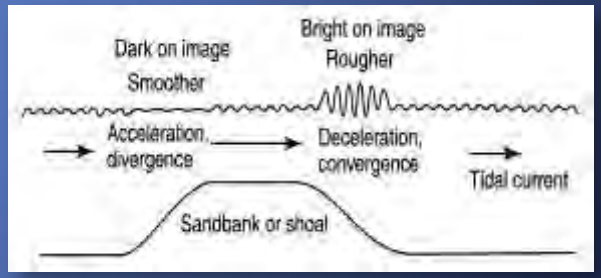

[Robinson, 2003]

ERS-1 SAR Image (C-VV, 100 km × 100 km)
Chinese Coast
(8 July 1995, 0234 UTC, © ESA)

Bathymetry Maps from ATI Measurements

Airborne ATI-derived current vector field (German island of Sylt, experiments May 2001, 3.5 km × 3.5 km)

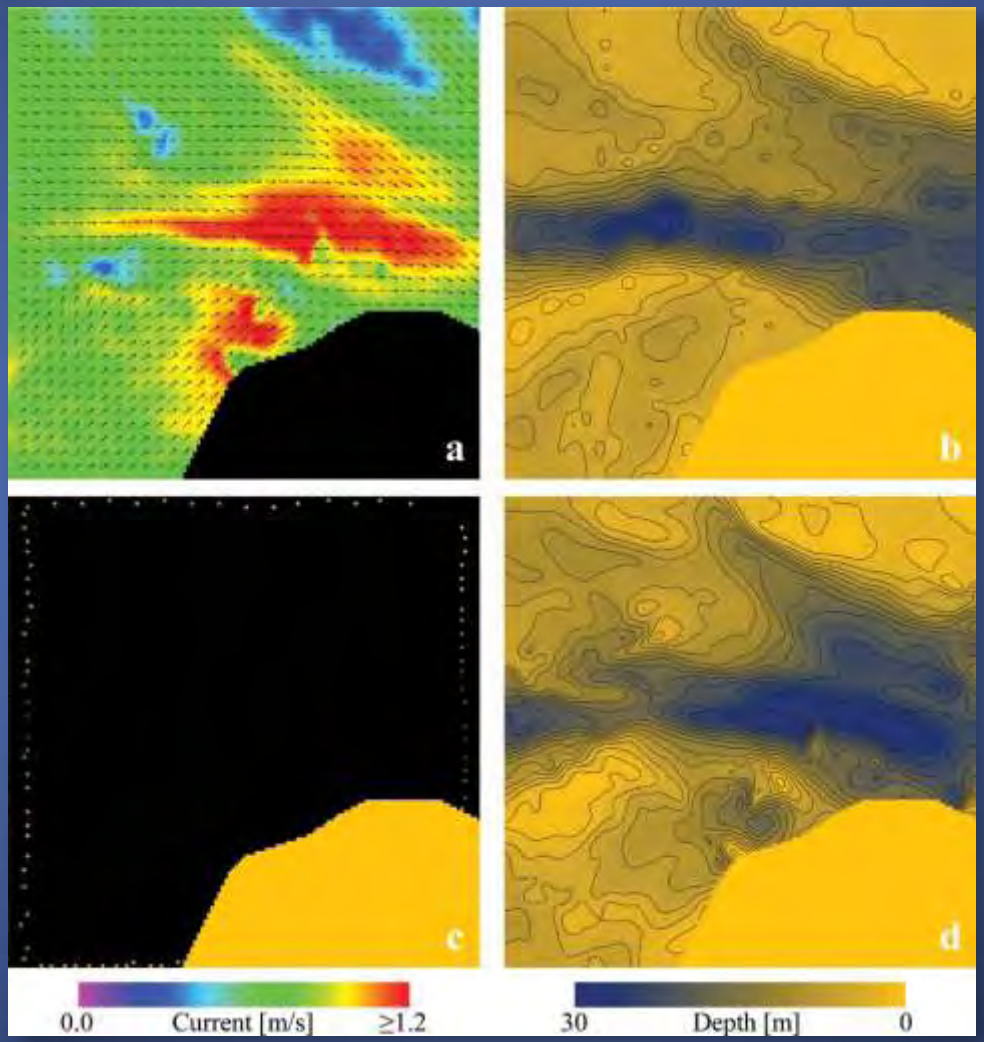

Depth map from echosoundings

Selected reference depth points

Depth map derived from reference points

[Romeiser, 2013]

Bathymetry Maps from Multiple SAR Imagery

Waterline Method

Extract waterlines from multiple SAR images acquired at different tidal phases (precise water levels needed)

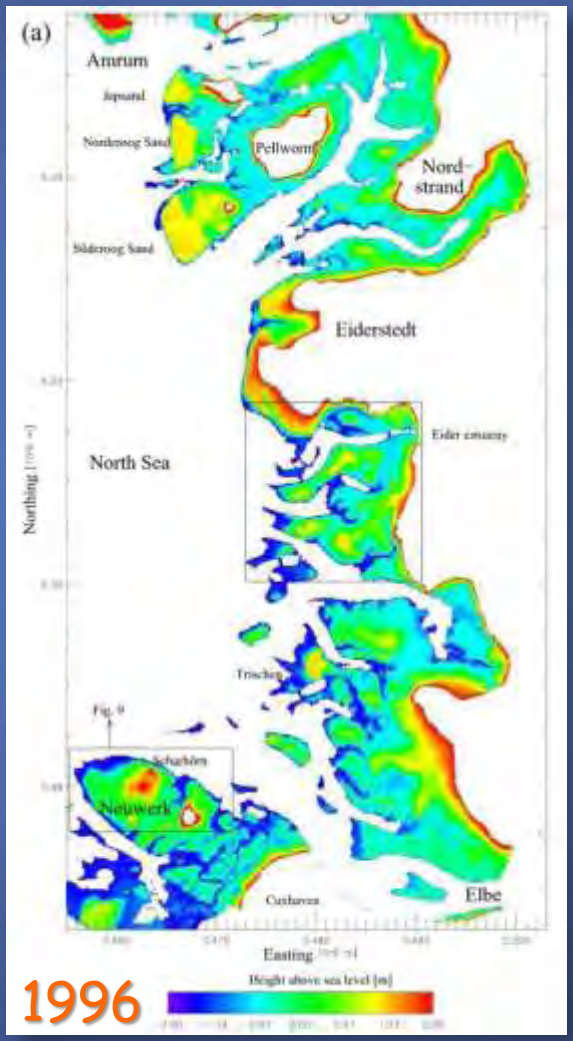

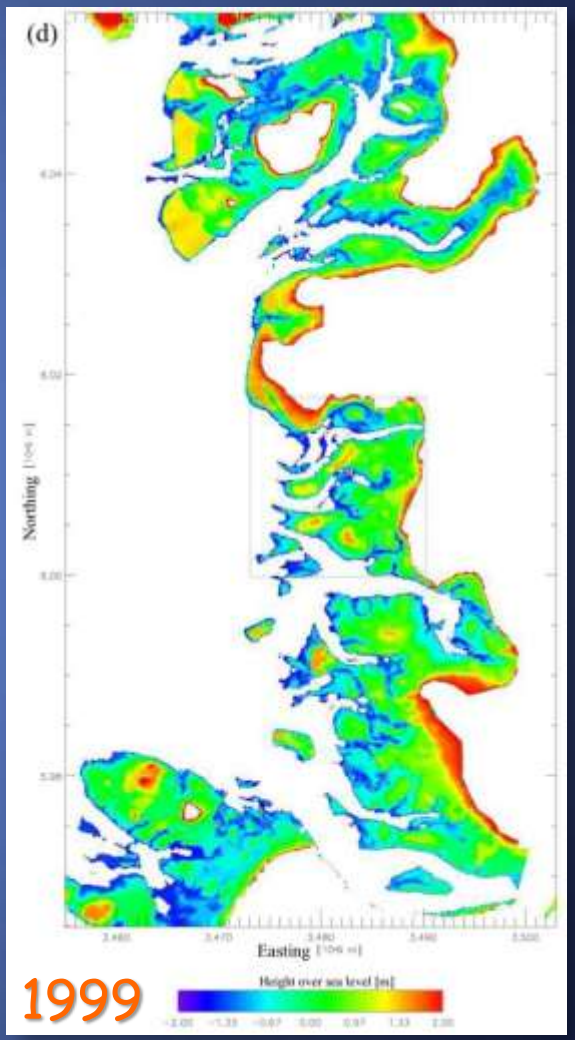

[Heygster et al., 2010]

Bathymetry Maps from Wave Statistics

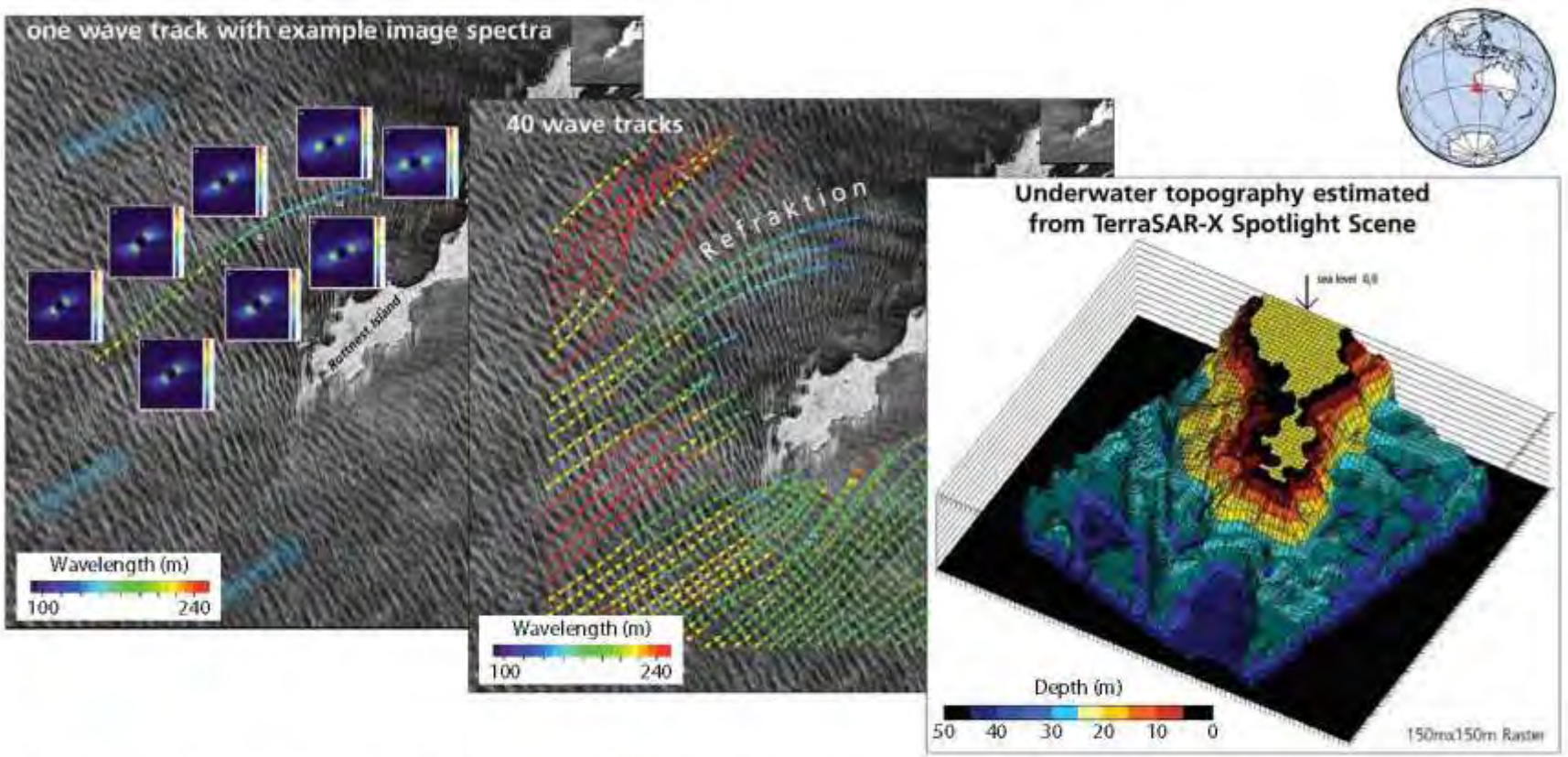

Figure 3. TerraSAR-X spotlight image (left) with dimensions of 10 km × 10 km and resolution of 1 m acquired over Rottenest Island, Australia, on October 20, 2009. (left) Normalized radar cross section (NRCS) and one wave track with example image spectra. (center) Forty wave rays (colored lines) tracked on the image. (right) Bathymetry (uniform raster, 150 m resolution) estimated from the TerraSAR-X image data. To complete the bathymetric maps in the shallowest areas (< 10 m water depth) near the coastline, optical data from the QuickBird satellite were used.

[Lehner et al., 2013]

Sea Bottom Topography
Take-Home Messages

Current variations: roughness variations
Current models (shallow waters)
Waterline method (intertidal flats)
Wave refraction (coasts)

Ship Detection

Radar Backscattering from Metal Constructions

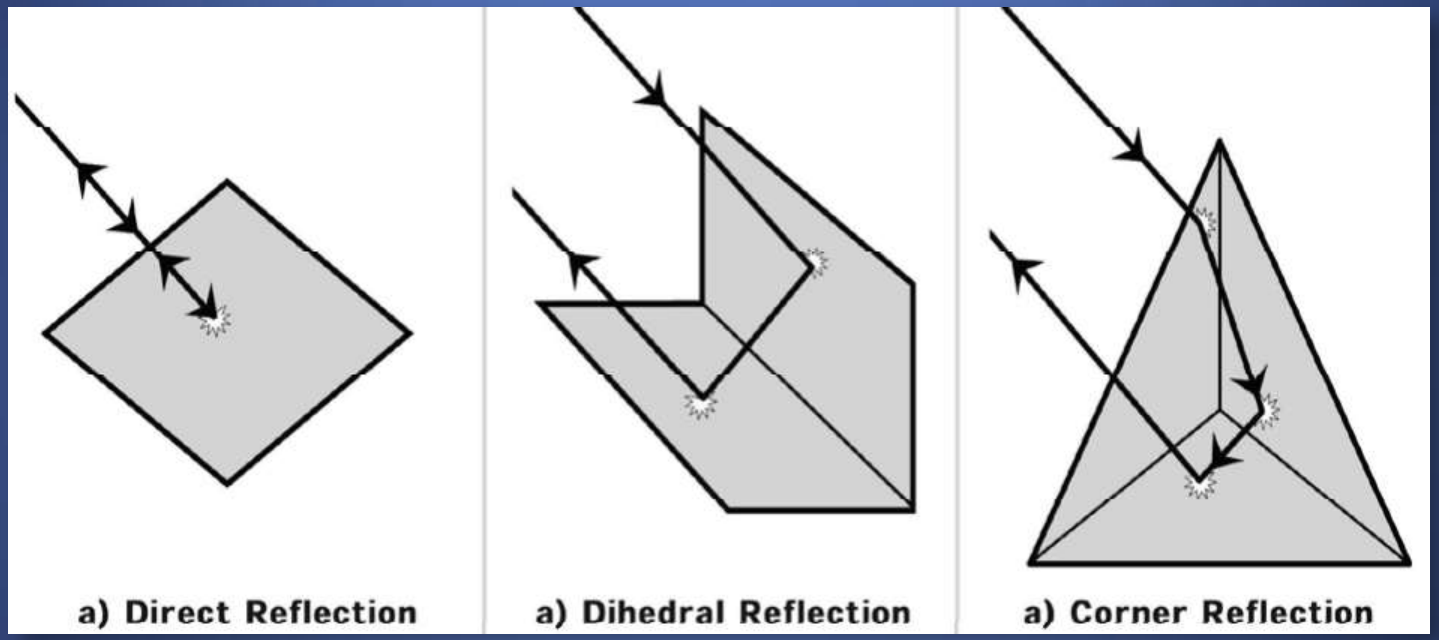

[Jackson & Apel, 2004]

Ship Wakes

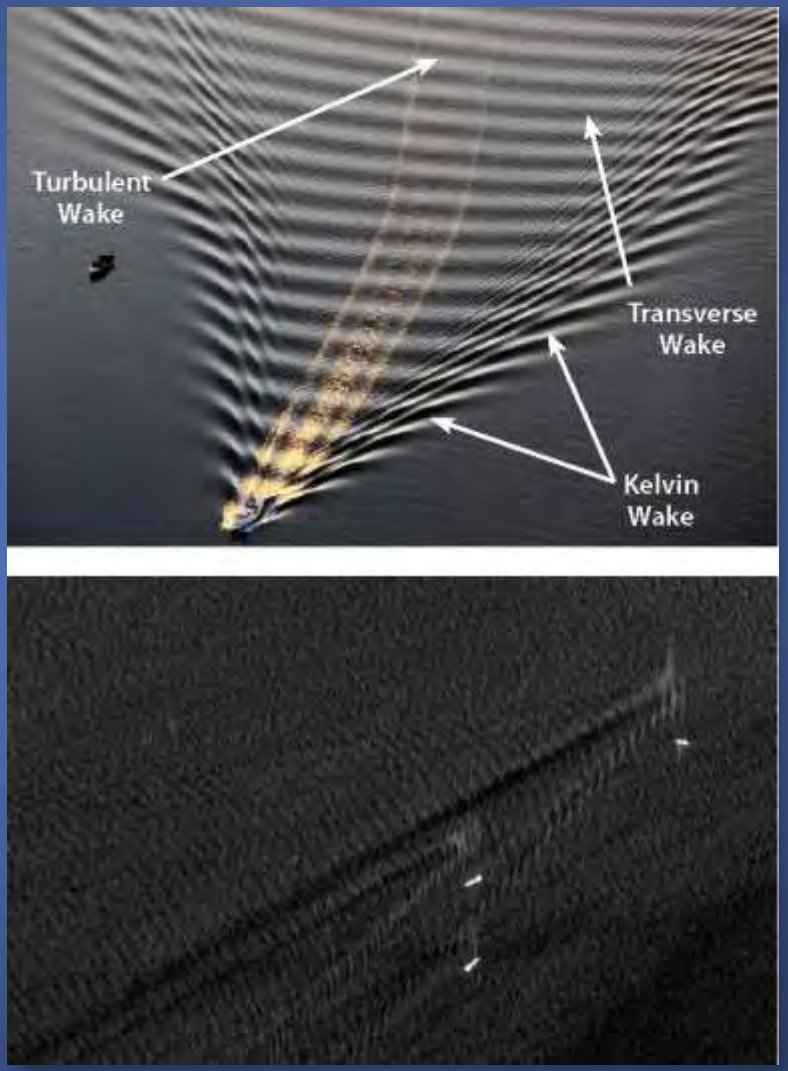

[Mallas & Graber, 2013]

Multi-Polarization SAR Imaging of Vessels

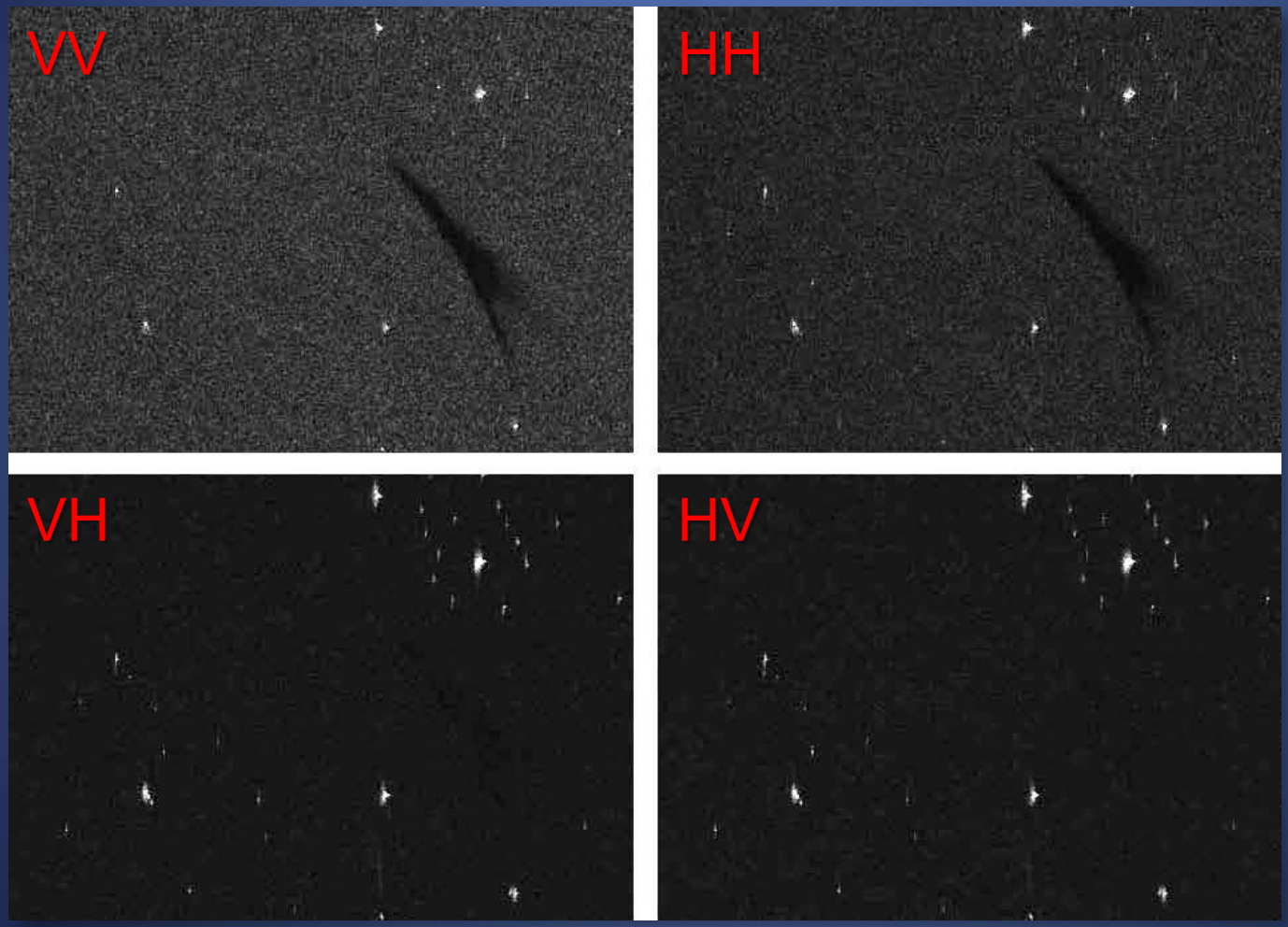

Radarsat-2 SAR Imagery (C), © CSA

[Mallas & Graber, 2013]

High-Resolution SAR Imaging of Large Vessels

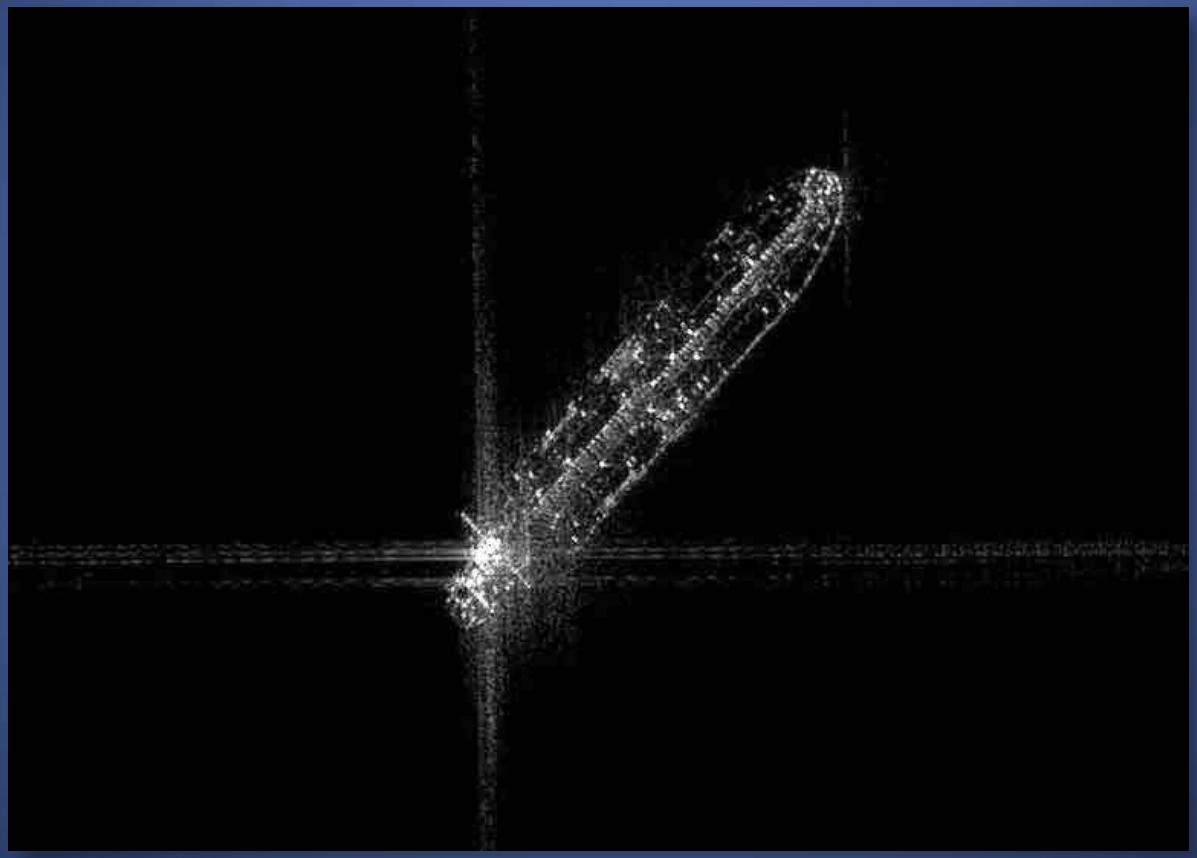

COSMO-SkyMed
SAR Image (X-VV)
© COSMO-SkyMed

[Mallas & Graber, 2013]

SAR Imaging of Hijacked Vessels

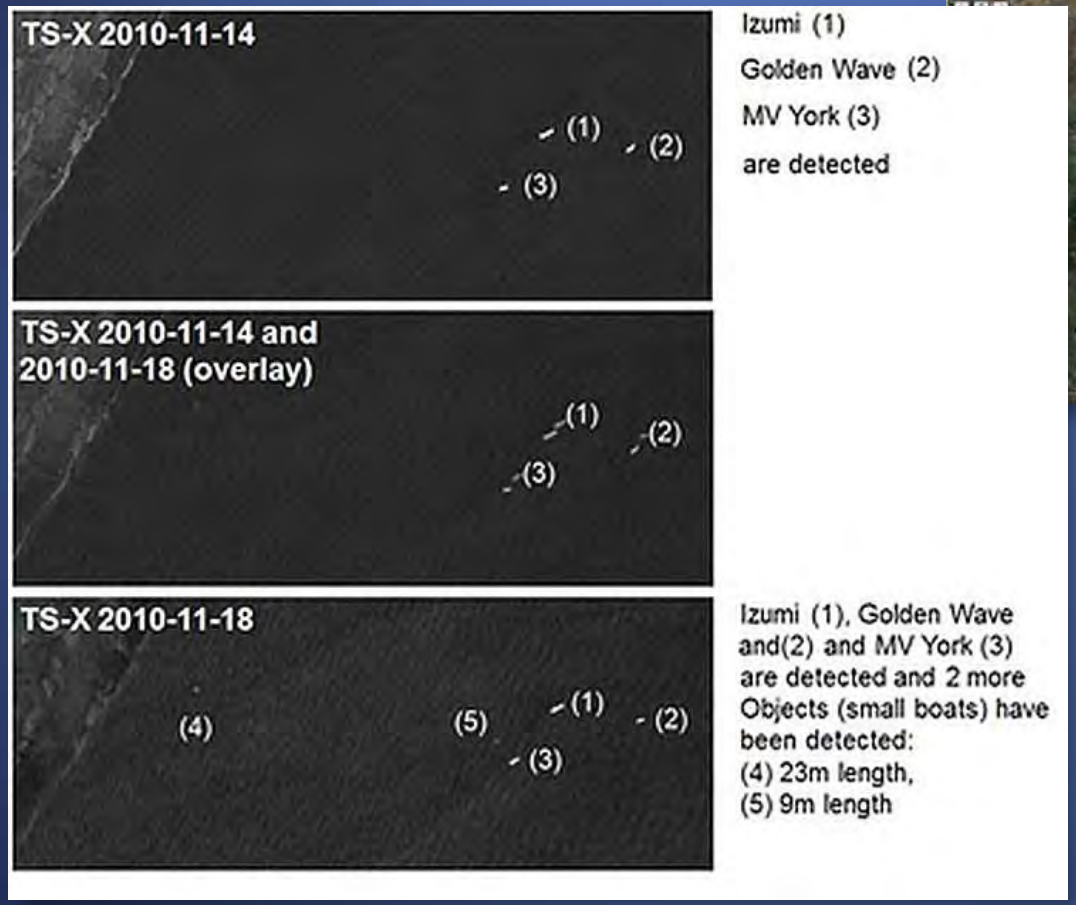

[Barale & Gade, 2014]

SAR Imaging of Vessels vs. AIS Info

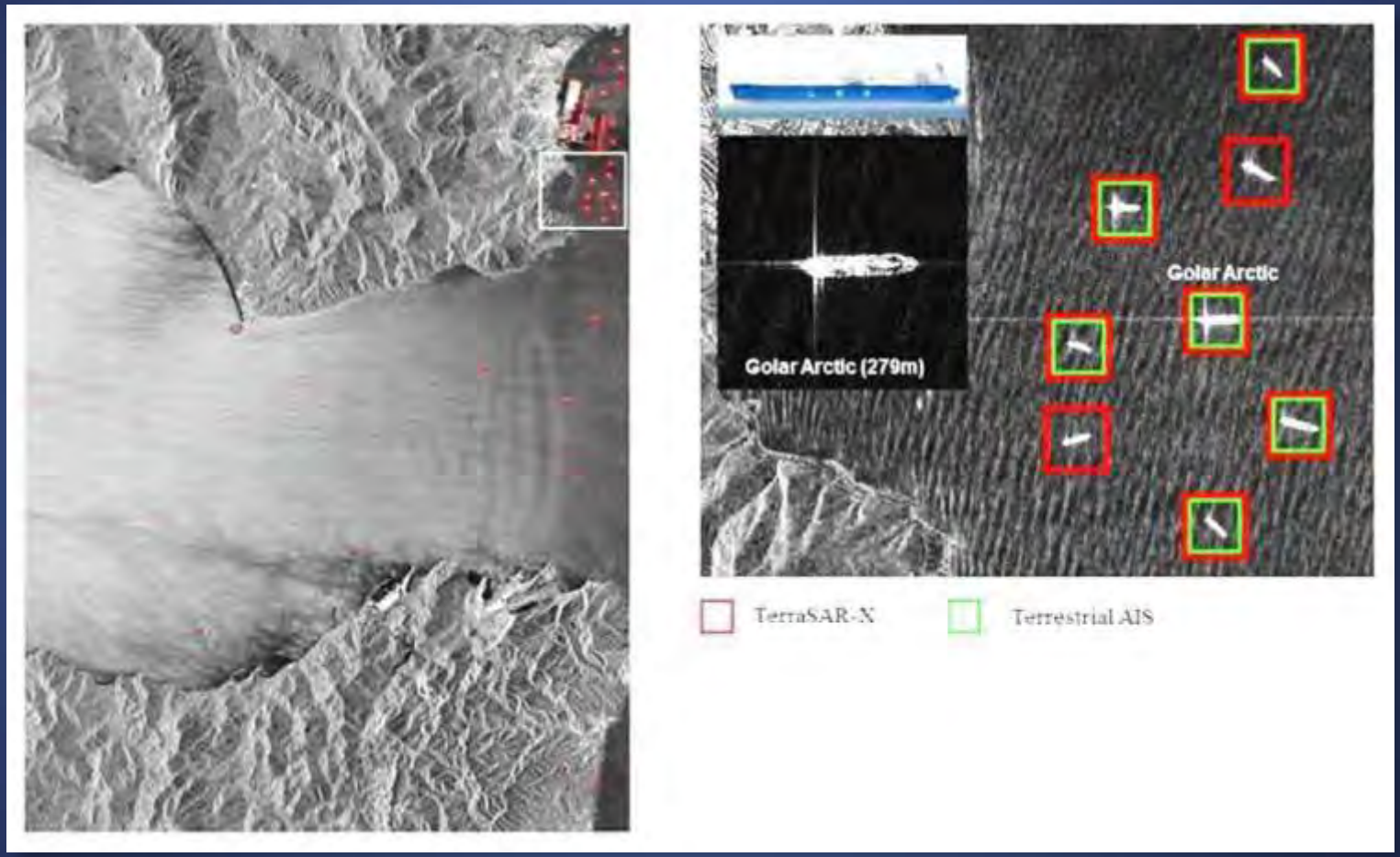

[Barale & Gade, 2014]

SAR Imaging of Marine Vessels

Speed estimate from azimuthal shift

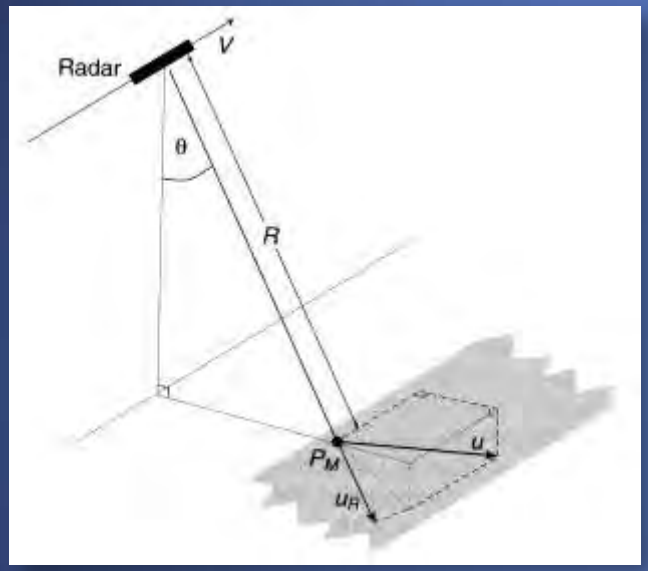

[Robinson, 2003]

$$f_D = -\frac{2u_R}{\lambda}$$

$$x_{am} = -\frac{u_R R}{V}$$

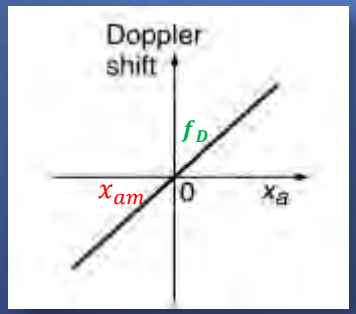

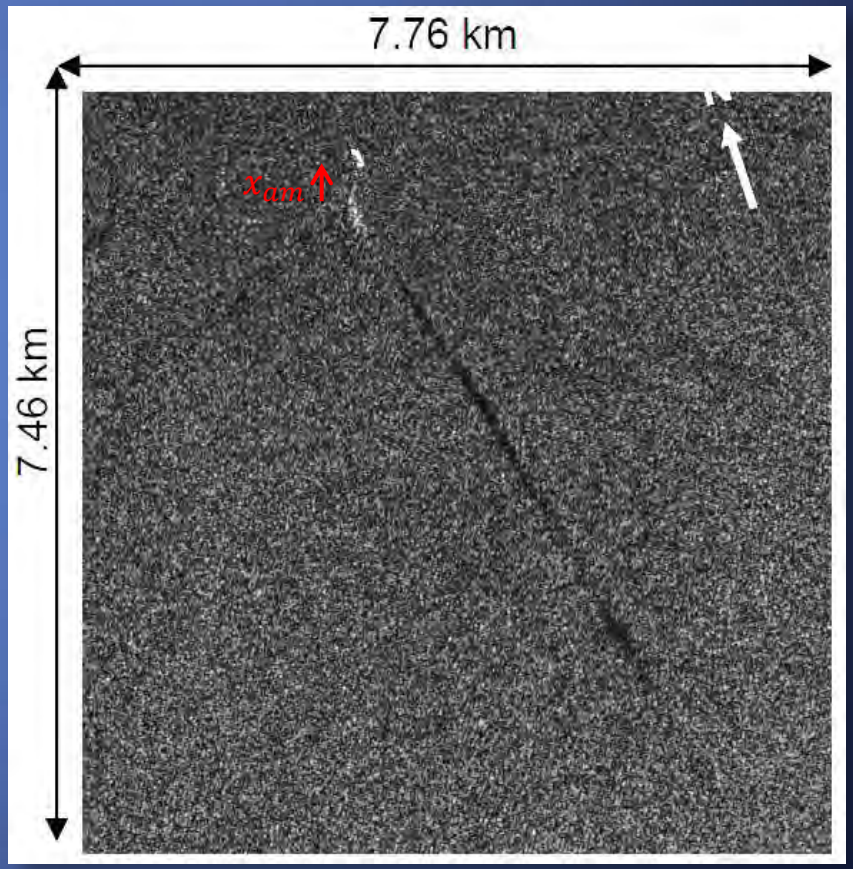

[Soloviev et al., 2008]

SAR Ambiguities ('Ghost Images')

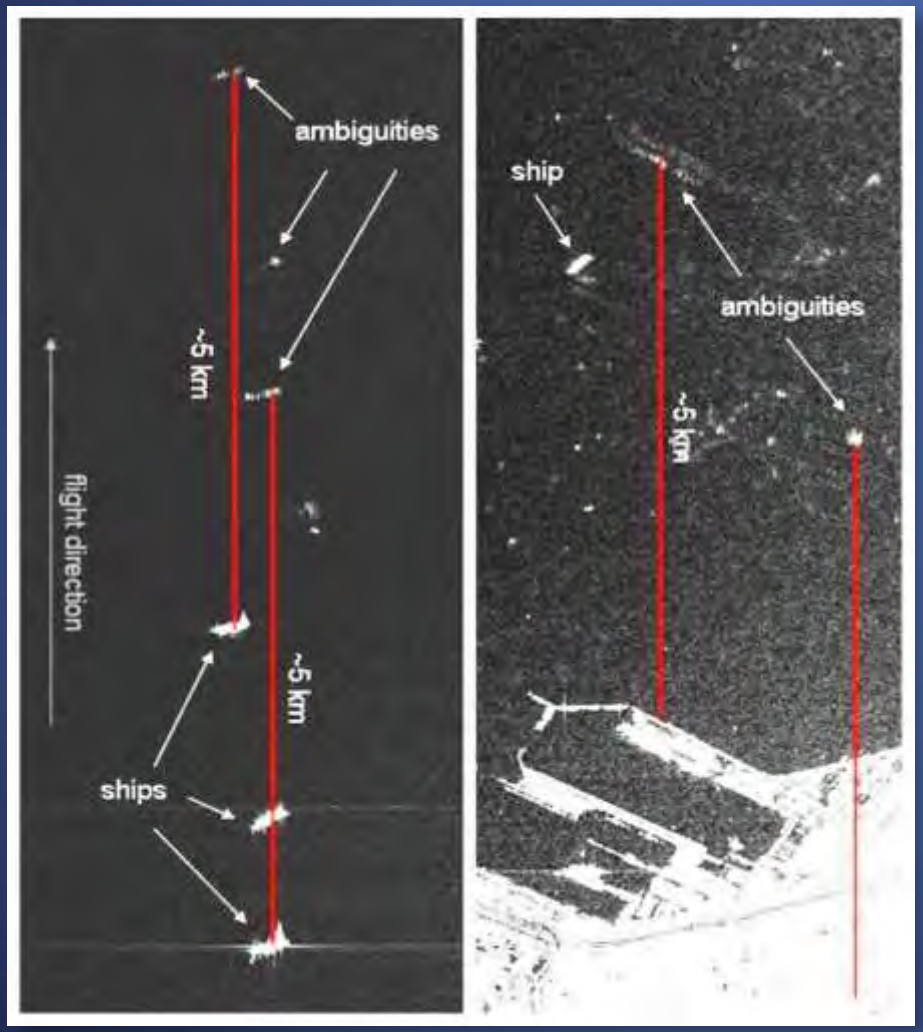

Ambiguity distance:

$$\Delta x = \Delta t_{AMBI} \cdot v_0 = \frac{PRF}{FM} \cdot v_0$$

PRF : pulse repetition frequency
FM : temporal derivative of Doppler frequency
v_0 : zero Doppler velocity

TerraSAR-X: Δx ≈ 5.2 km

[Barale & Gade, 2014]

Ship Detection
Take-Home Messages

High-resolution SAR used
Vessel monitoring (SAR vs. AIS)
Vessel speeds ("ship-off-the-track")

Oil Pollution Monitoring

SAR Monitoring of Marine Oil Pollution

Operation Oil Pollution

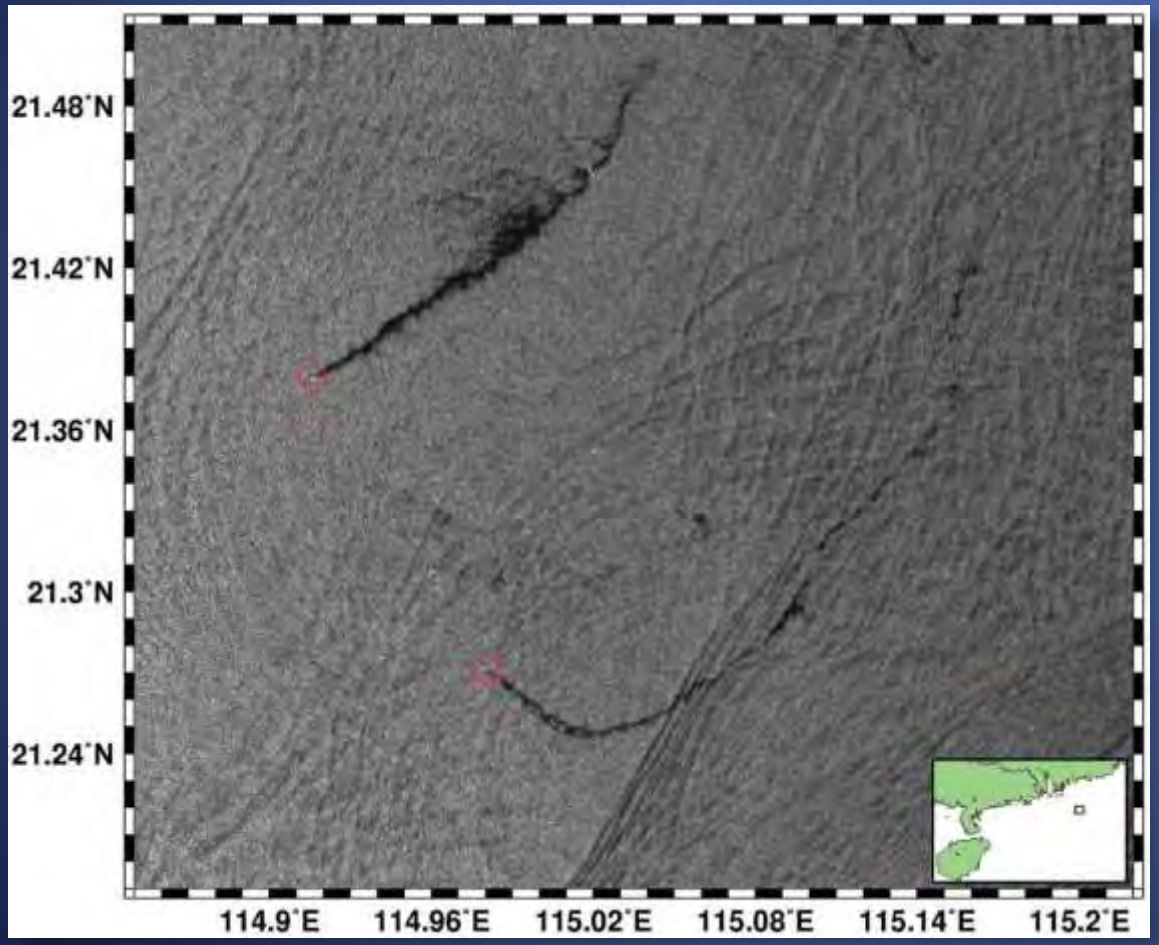

ERS SAR Image (C-VV, 50 km × 50 km)
South China Sea
(25 May 2007, 14:44 UTC, © ESA)

[Caruso et al., 2013]

SAR Monitoring of Marine Oil Pollution

Accidential Oil Pollution

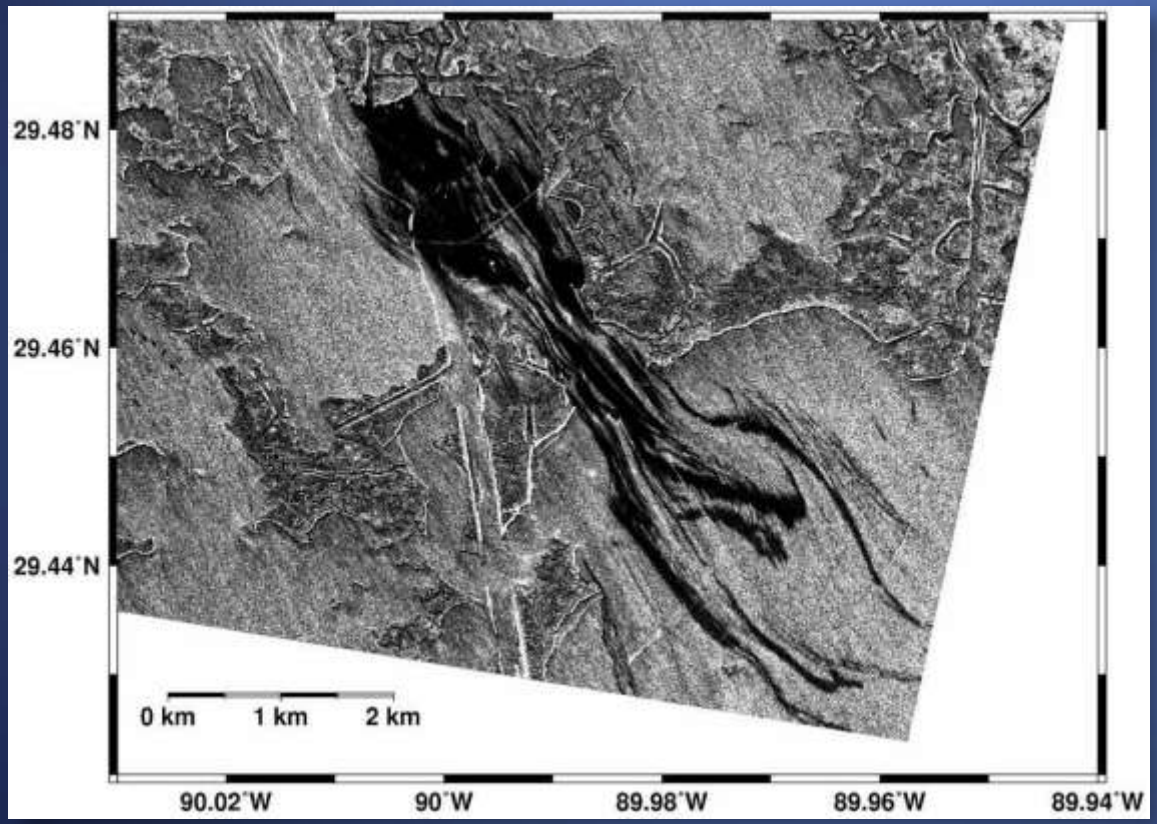

Wellhead struck by tugboat *Pere Ana C.*

TerraSAR-X Image (X-VV)
Mud Lake, LA, USA
(1 August 2010, 12:08 UTC, © DLR)

[Caruso et al., 2013]

SAR Monitoring of Marine Oil Pollution

Accidential Oil Pollution

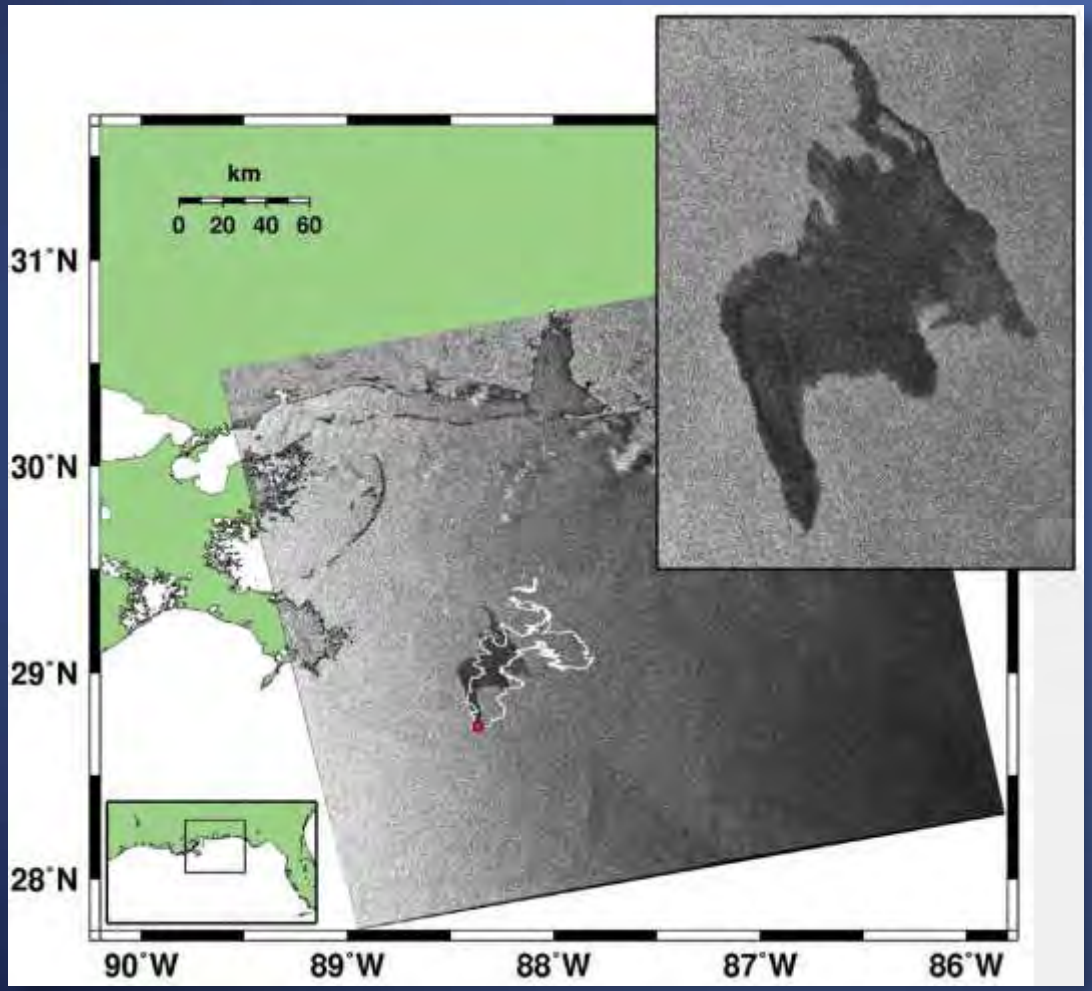

Deepwater Horizon (●) incident

TerraSAR-X Image (X-VV)
Gulf of Mexico
(23 April 2010, 12:08 UTC, © DLR)

Extent on 25 April 2010:

[Caruso et al., 2013]

SAR Image Examples

ERS-2 SAR Images (C-VV, 30 km × 40 km)
Northwestern Mediterranean Sea
(© ESA)

SAR Applications

Oil pollution in European marginal seas (1996-99)

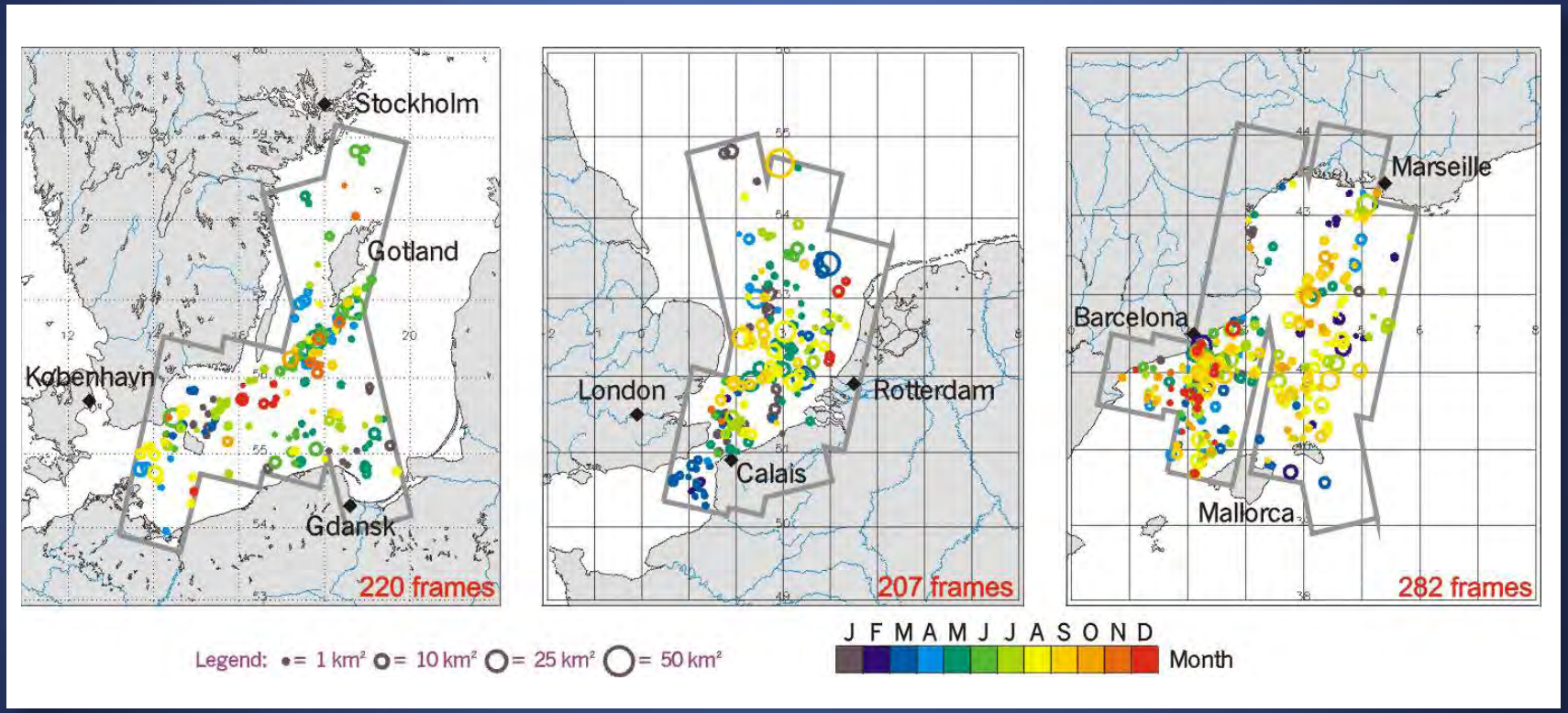

SAR Applications

Mean oil pollution of the Mediterranea Sea 1999-2004

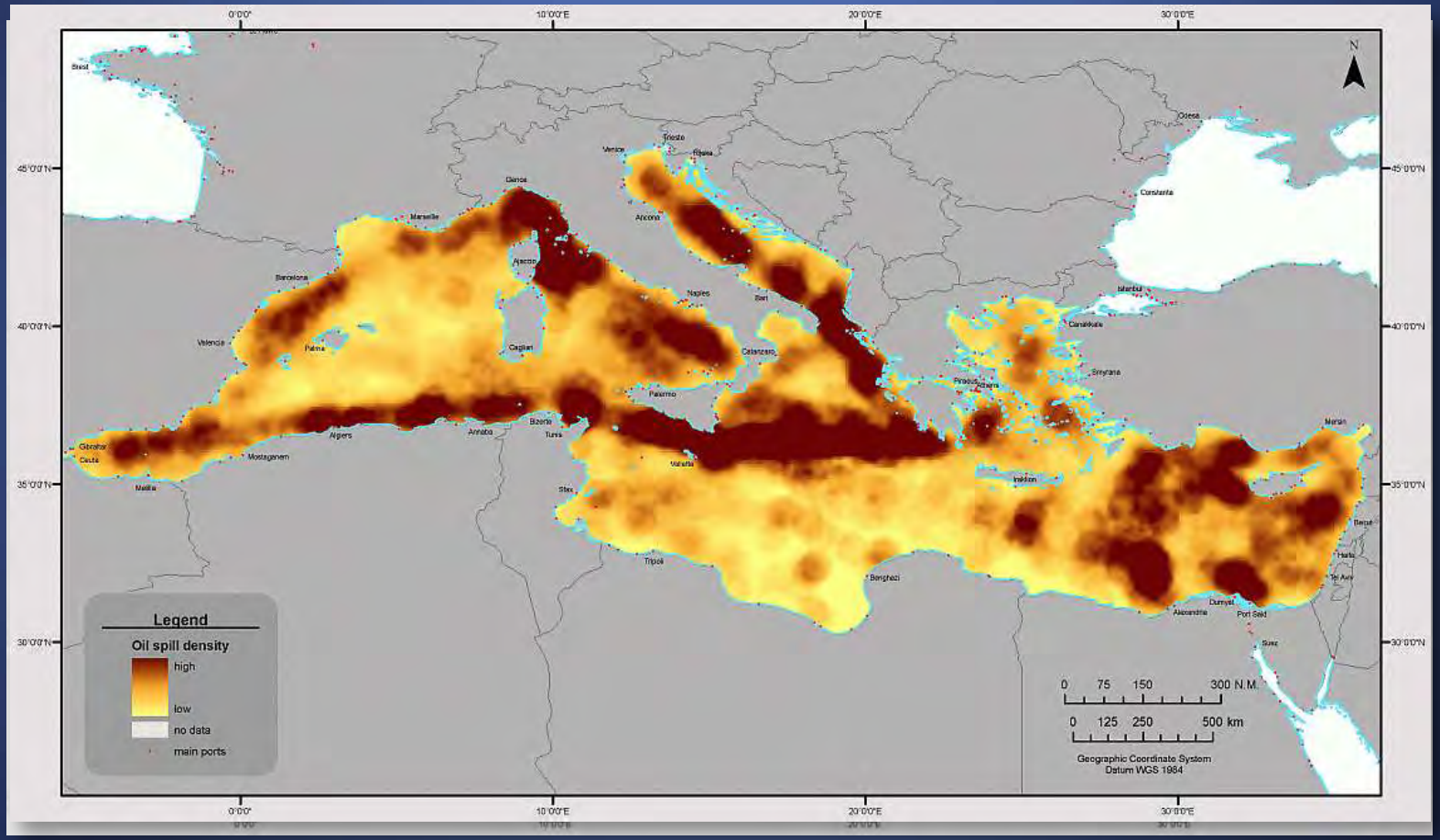

[Barale & Gade 2008]

Wave Damping by Surface Films

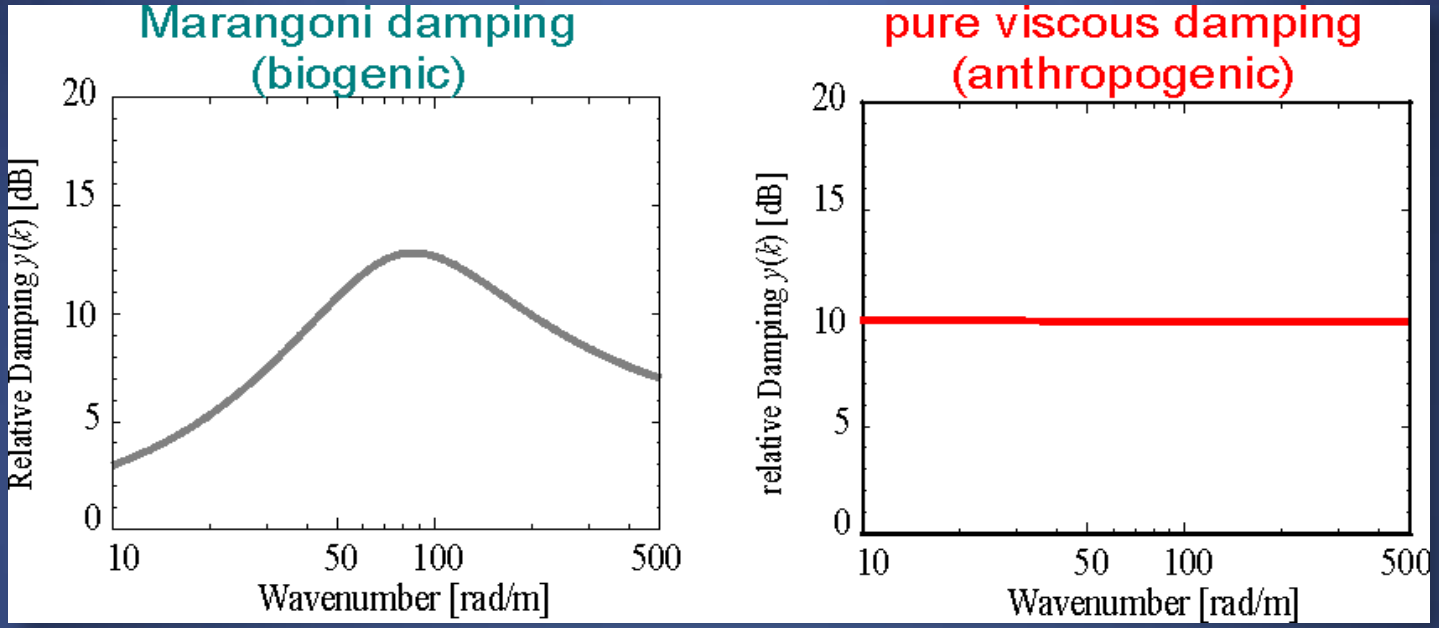

Use multi-frequency radar techniques to discriminate between biogenic and anthropogenic surface films

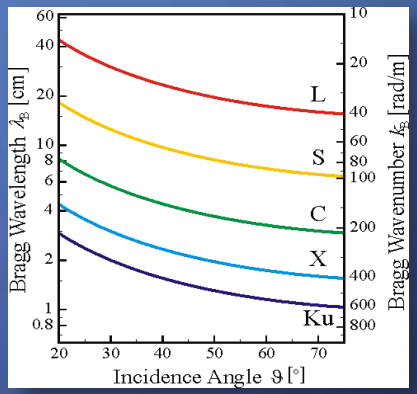

Scatterometer Experiments

MULTI³SCAT of Uni Hamburg

- flown on BO 105
- 5 frequencies: (L, S, C, X, Ku band)
- 4 polarisations (HH, HV, VV, VH)
- incidence angle: 23° ... 65°
- nominal flight height: 150 m
- Ø footprint: 1.6 m ... 128.9 m
- transmit power: 10 mW ... 150 mW

Field Experiments With Marine Surface Films

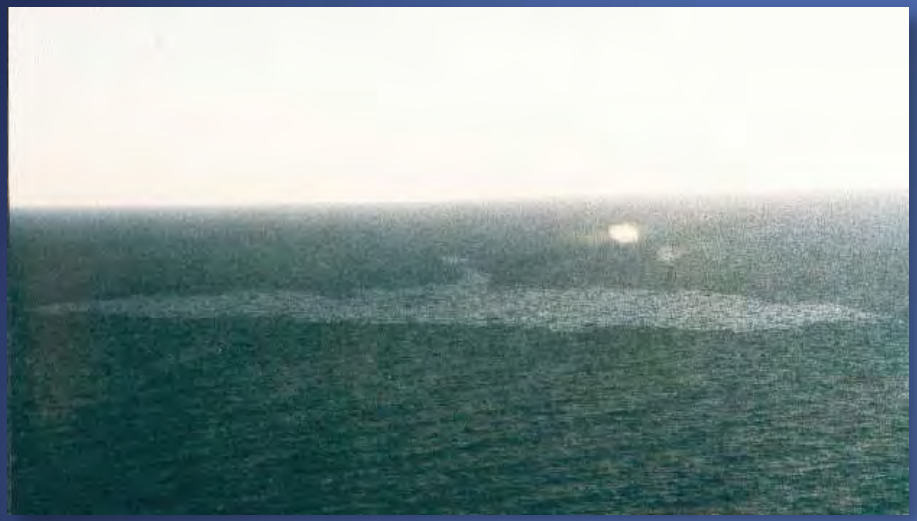

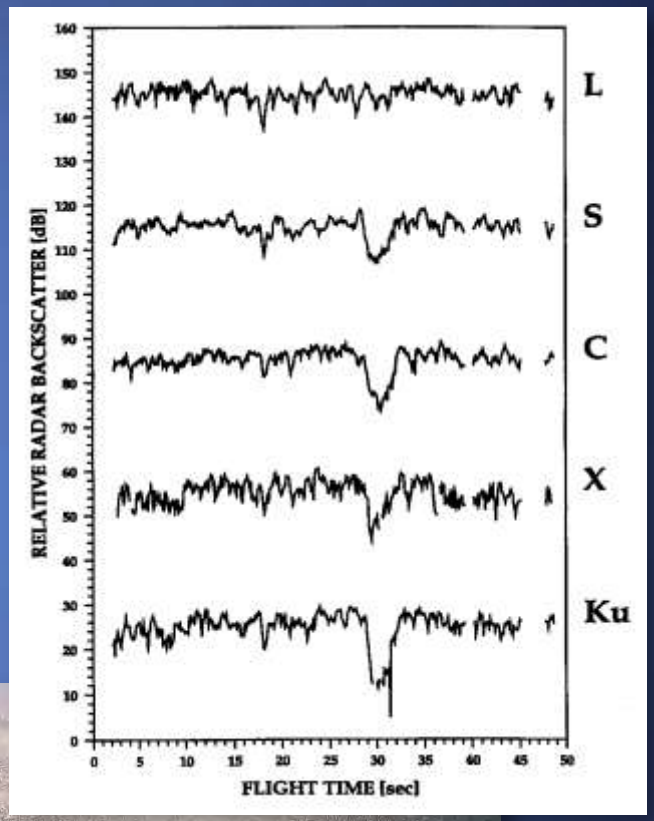

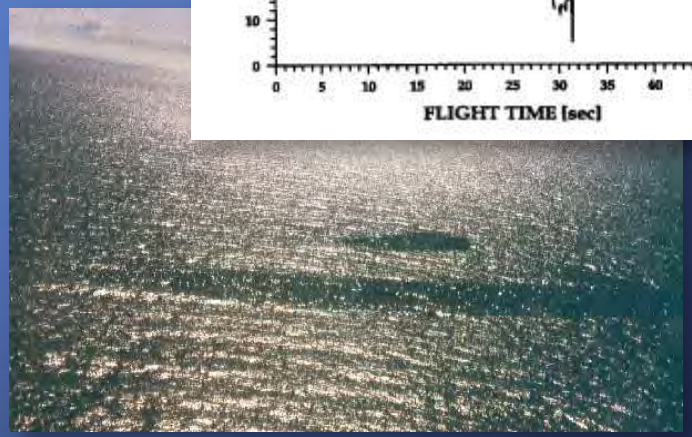

Field Experiments With Marine Surface Films

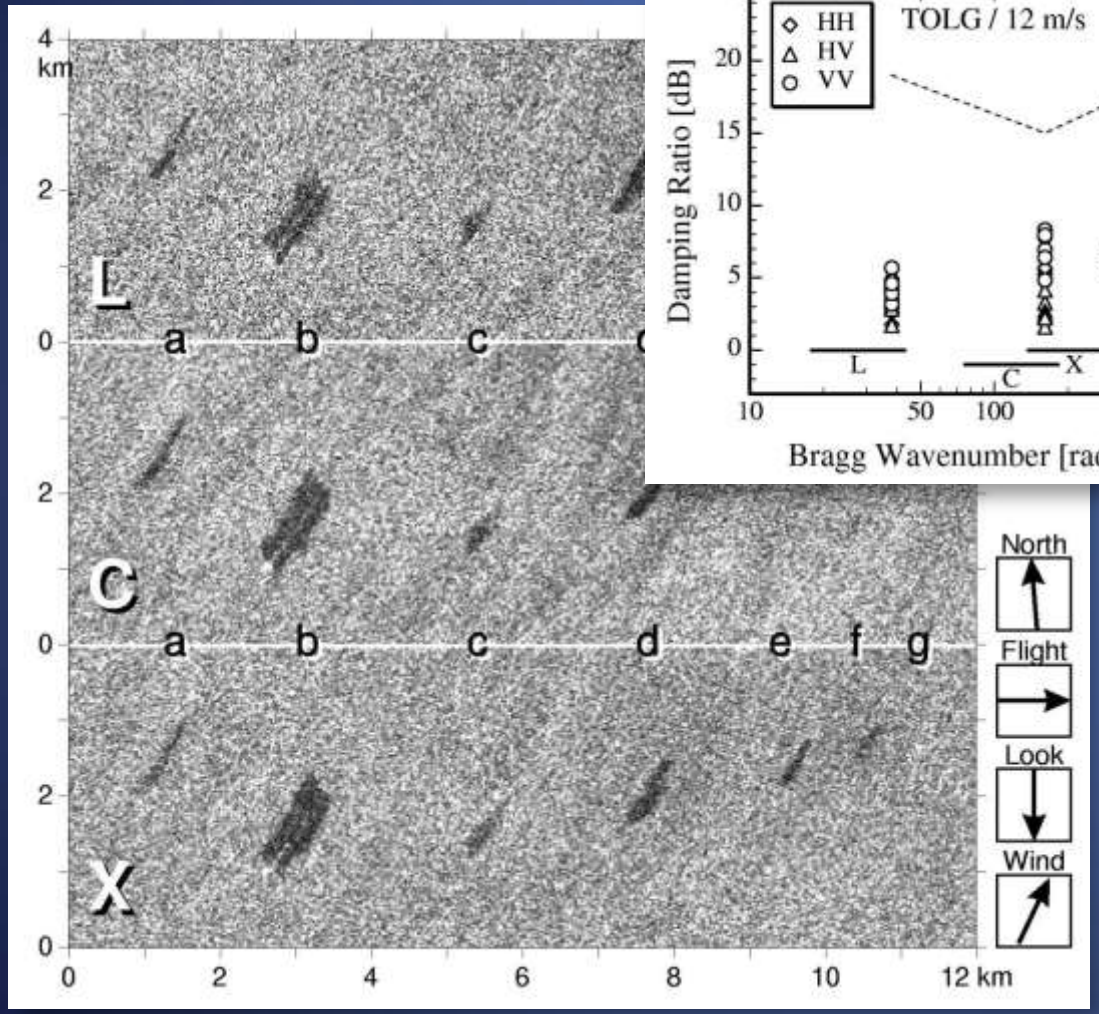

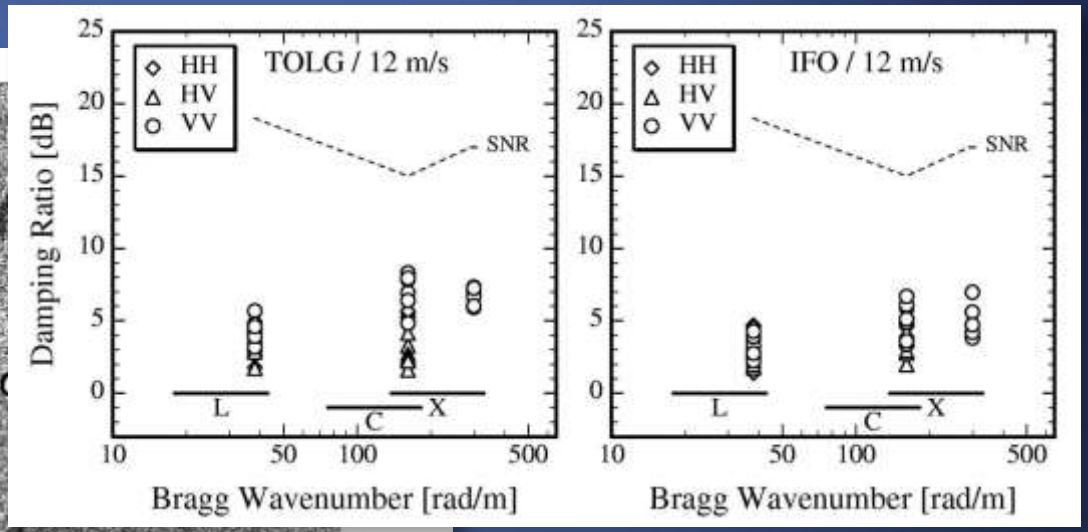

1994: 2 SIR-C/X-SAR missions

Field experiments with quasi-biogenic slicks and anthropogenic oil spills

Just minor differences in radar contrast at high wind speeds (12 m/s)

Field Experiments With Marine Surface Films

Modeling damping ratios at high wind speeds

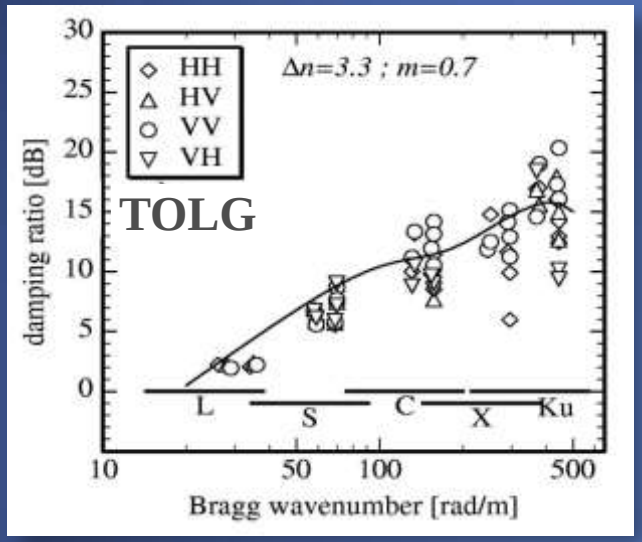

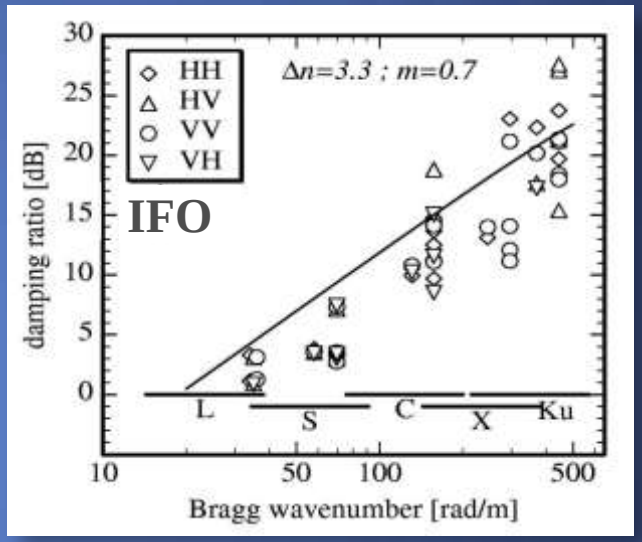

[Gade, 1996]

$$\frac{\sigma^{(0)}}{\sigma^{(s)}} = \frac{\Psi_0(k)}{\Psi_s(k)} \approx \frac{\beta_s - 2\Delta_s c_g}{\beta_0 - 2\Delta_0 c_g} \cdot m^{\Delta n - 4} \left(2u_* \sqrt{\frac{|\cos\varphi| k}{g}} \right)^{\Delta n}$$

m : parameter describing reduction of friction velocity
Δn : parameter describing reduction of wave breaking

Model can explain

monotonous increase of damping curves (no Marangoni maximum!)

similar damping behavior of biogenic and anthropogenic films

SAR Oil Detection System

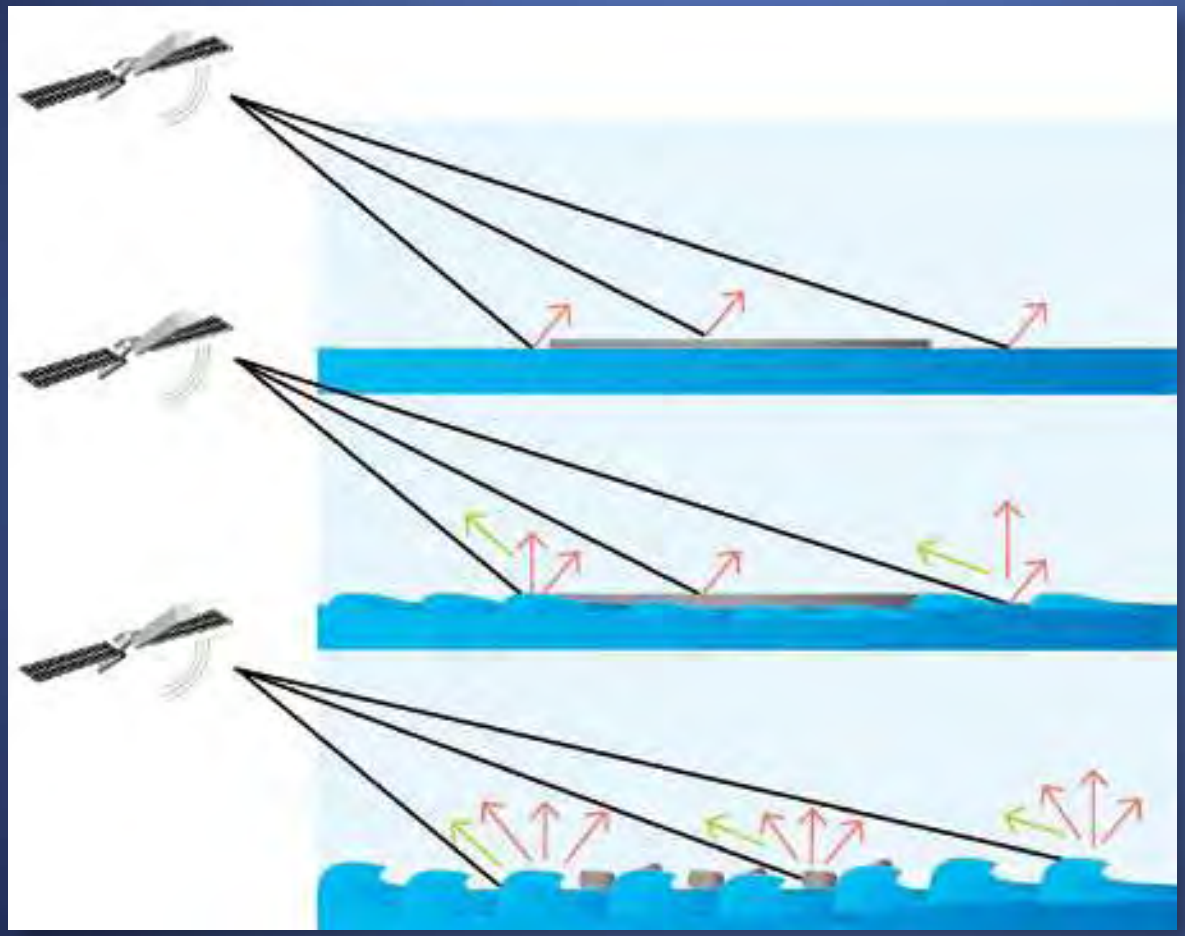

Low wind

Moderate wind

High wind

[EMSA, 2014]

Wind-Speed Dependence of Radar Contrast

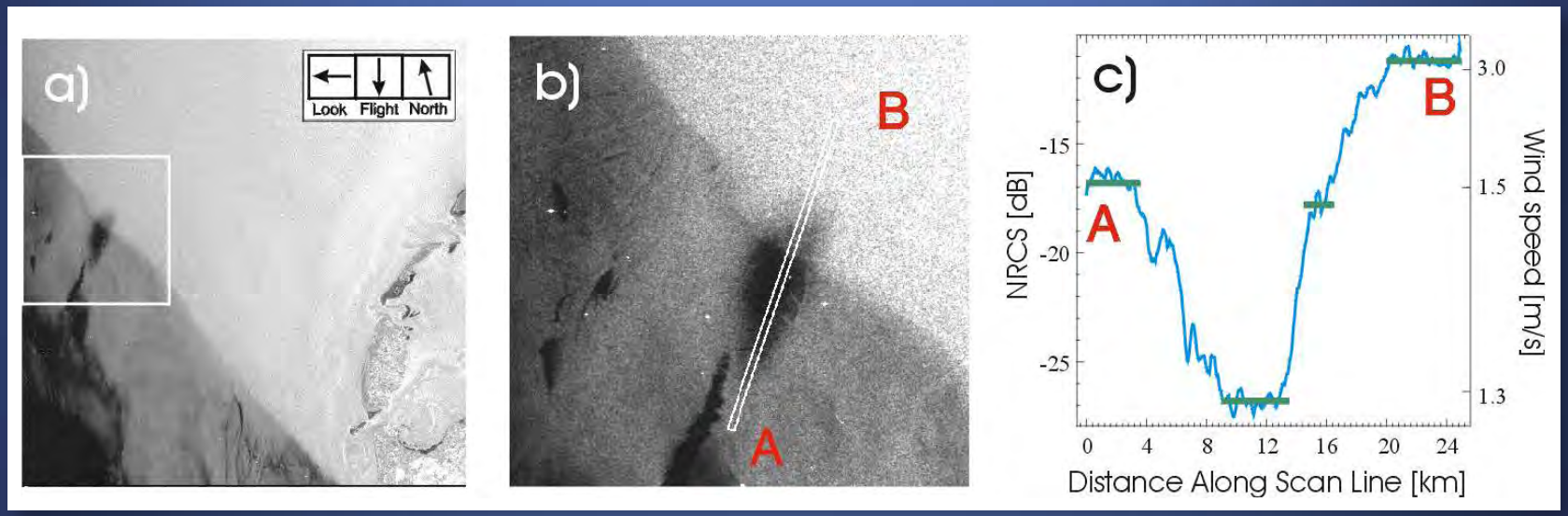

ERS-2 SAR image (C-VV, 100 km 100 km)
North Sea
24 March 1997, 10:40 UTC, © ESA

Statistical Analyses

Normalized Visibility

Defined as ratio A/B of the wind speed distribution of detected oil spills (A) and model winds (B)

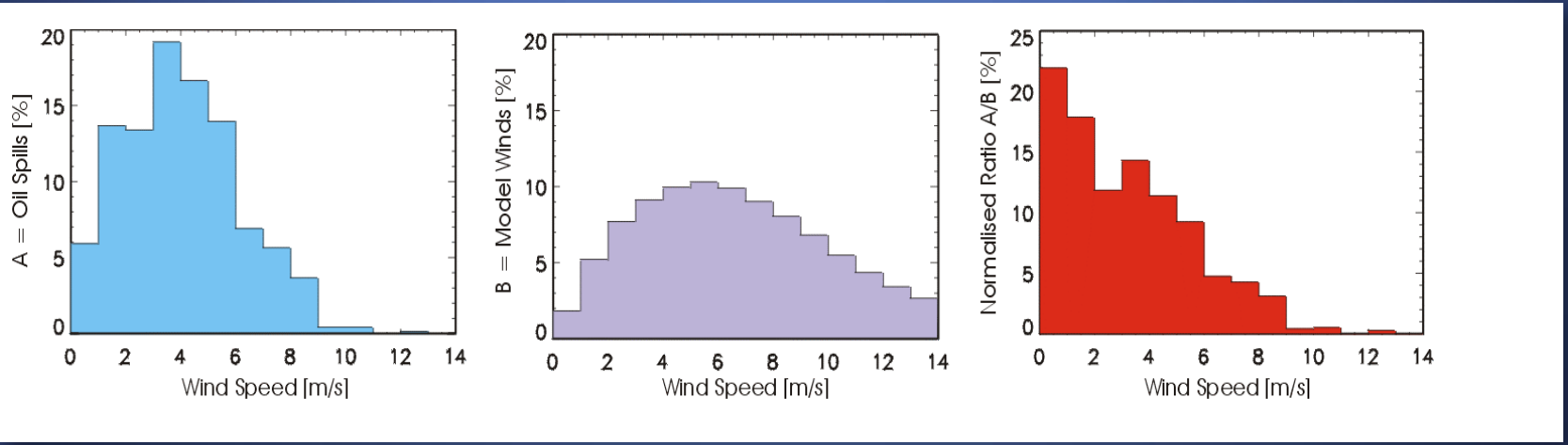

Any oil pollution in the three 'Clean Seas' test sites is visible only at wind speeds up to 9-10 m/s !

SAR Oil Detection System

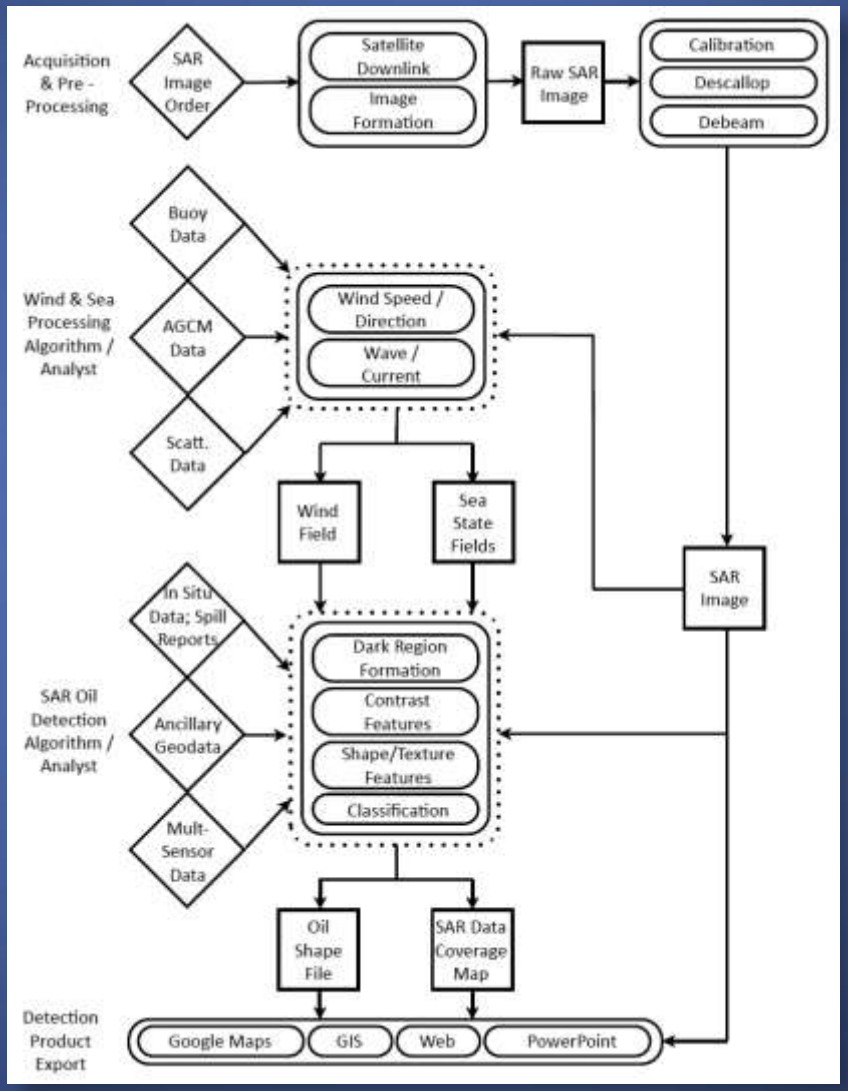

[Caruso et al., 2013]

Oil Pollution Monitoring
Take-Home Messages

Routine monitoring, pollution statistics
Oil-cleanup support
Detection @ 2 m/s - 10 m/s

Sea Ice

Sea Ice

Roughness scales and volume inclusion

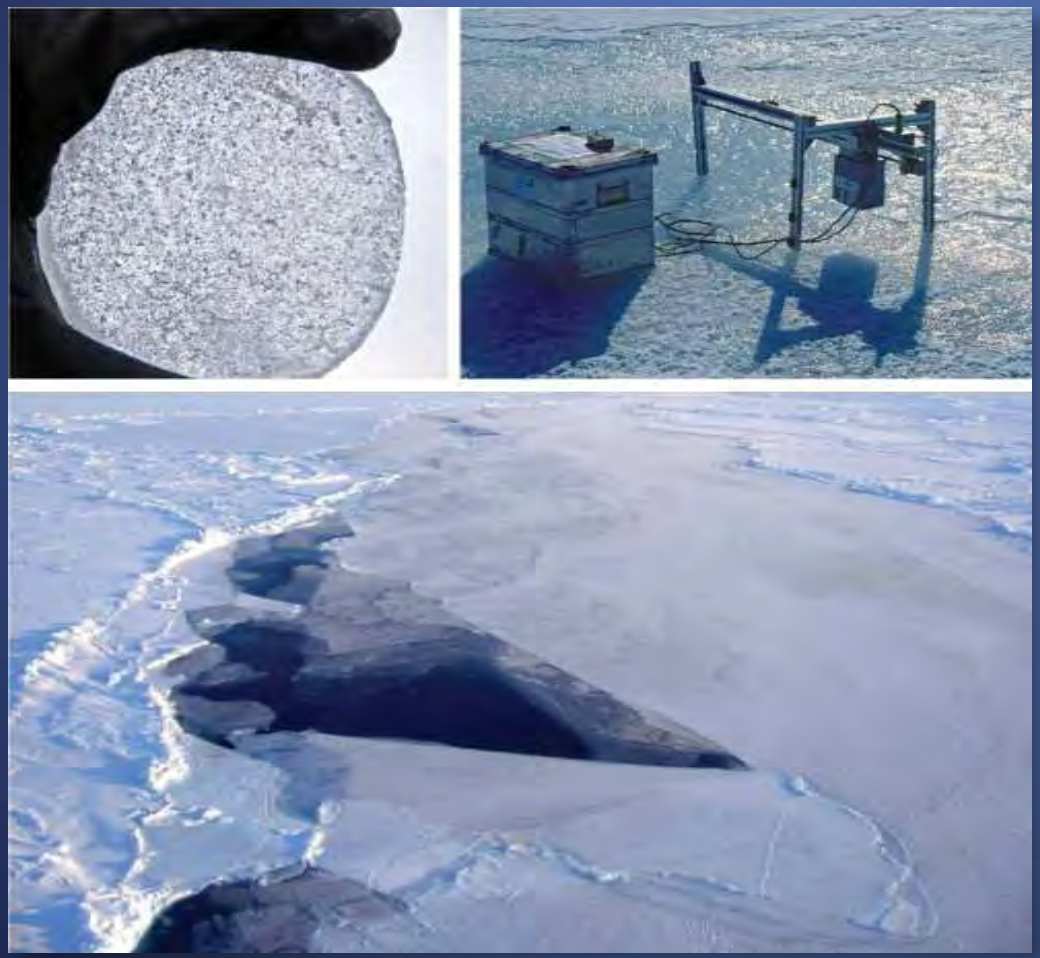

Left: Air bubbles in Baltic first-year ice (ice slab diameter 8 cm)

Right: Small-scale ripples on sea ice (laser measurements in the Baltic)

Left: Deformed sea ice in the Fram Strait (refrozen lead with rafted thin ice; thicker, ridged ice)

[Dierking 2013]

Remote Sensing of Sea Ice

Comparison of optical and SAR imagery (N Svålbard)

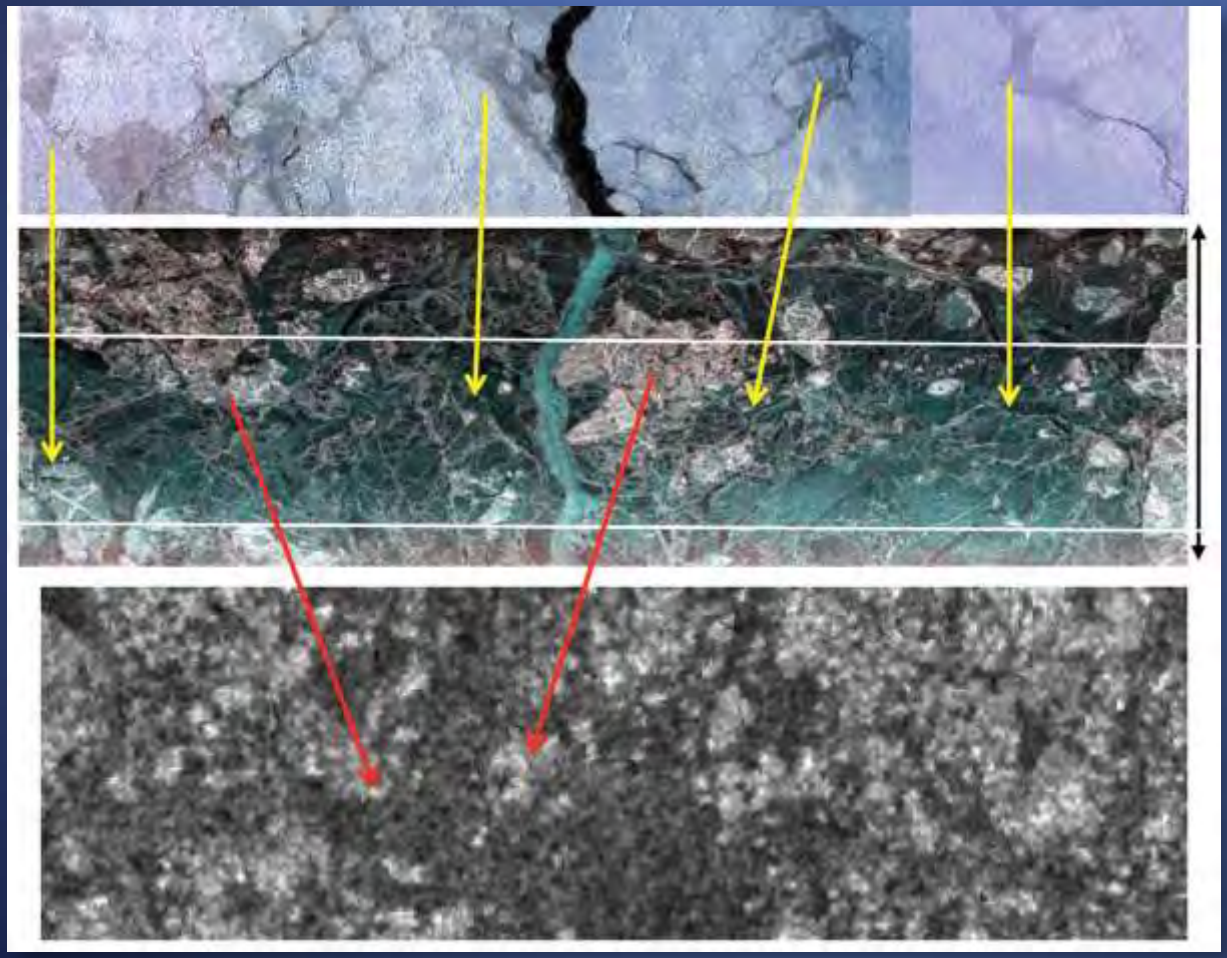

Airborne optical imager
19 March 2007, 12:20 UTC
spatial resolution < 1.3 m

Airborne SAR sensor
ESAR (DLR)
19 March 2007, 12:26 UTC
spatial resolution 2 m

Spaceborne SAR sensor
ENVISAT ASAR WS (C-HH)
19 March 2007, 11:22 UTC
spatial resolution 150 m

[Dierking 2013]

Remote Sensing of Sea Ice

Influence of melting conditions (Beaufort Sea)

ENVISAT ASAR images (C-HH, 90 km × 90 km, 19° < θ < 28°), © ESA

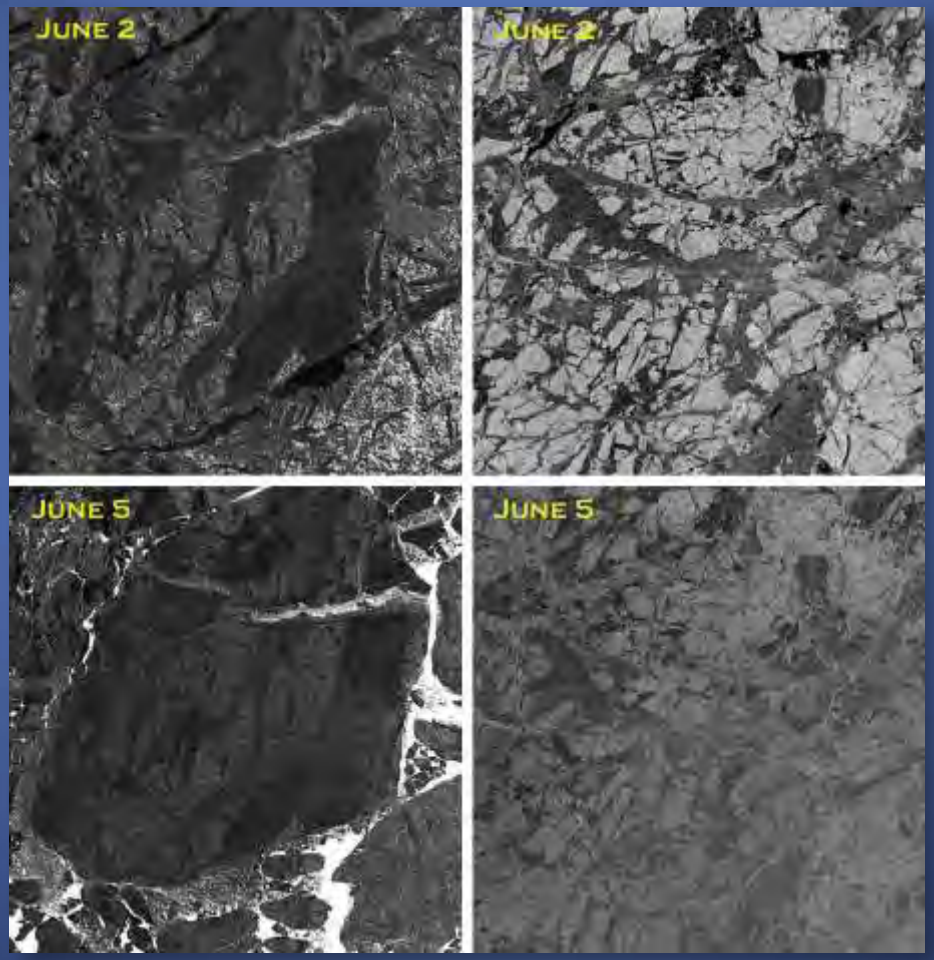

ENVISAT ASAR images (C-HH, 90 km × 90 km, 35° < θ < 43°), © ESA

[Dierking 2013]

SAR Imaging of Sea Ice

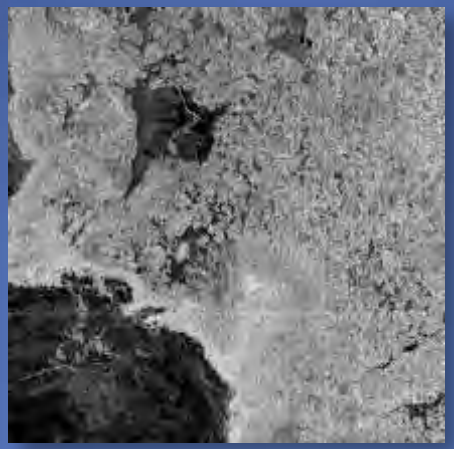

SAR images (80 km × 80 km)
Arctic sea ice at 82°N 12°E
(19 September 1996, © ESA, CSA)
left: ERS (C Band, VV pol)
right: Radarsat (C Band, HH pol)

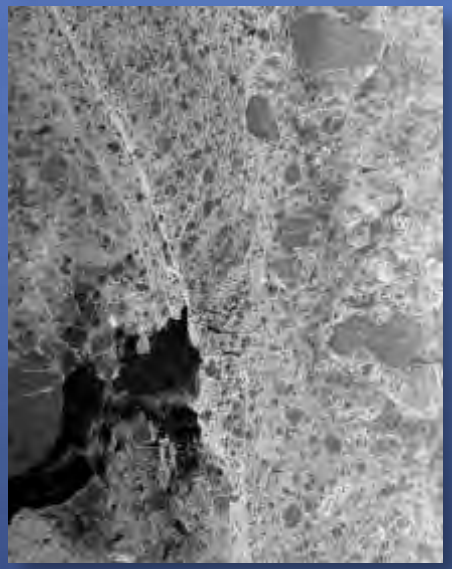

ERS SAR image (50 km × 65 km)
Arctic sea ice
(© ESA, NASDA)
left: ERS (C Band, VV pol)
right: JERS-1 (L Band, HH pol)

[Barale & Gade 2008]

Remote Sensing of Sea Ice

Ice-drift vectors derived from SAR imagery

ENVISAT ASAR images (C-HH)
Ronne Polynya, Wedell Sea
© ESA

18 February 2008, 06:09 UTC

19 February 2008, 05:38 UTC

Drift vectors from SAR image analysis (red) and visual inspection (yellow)

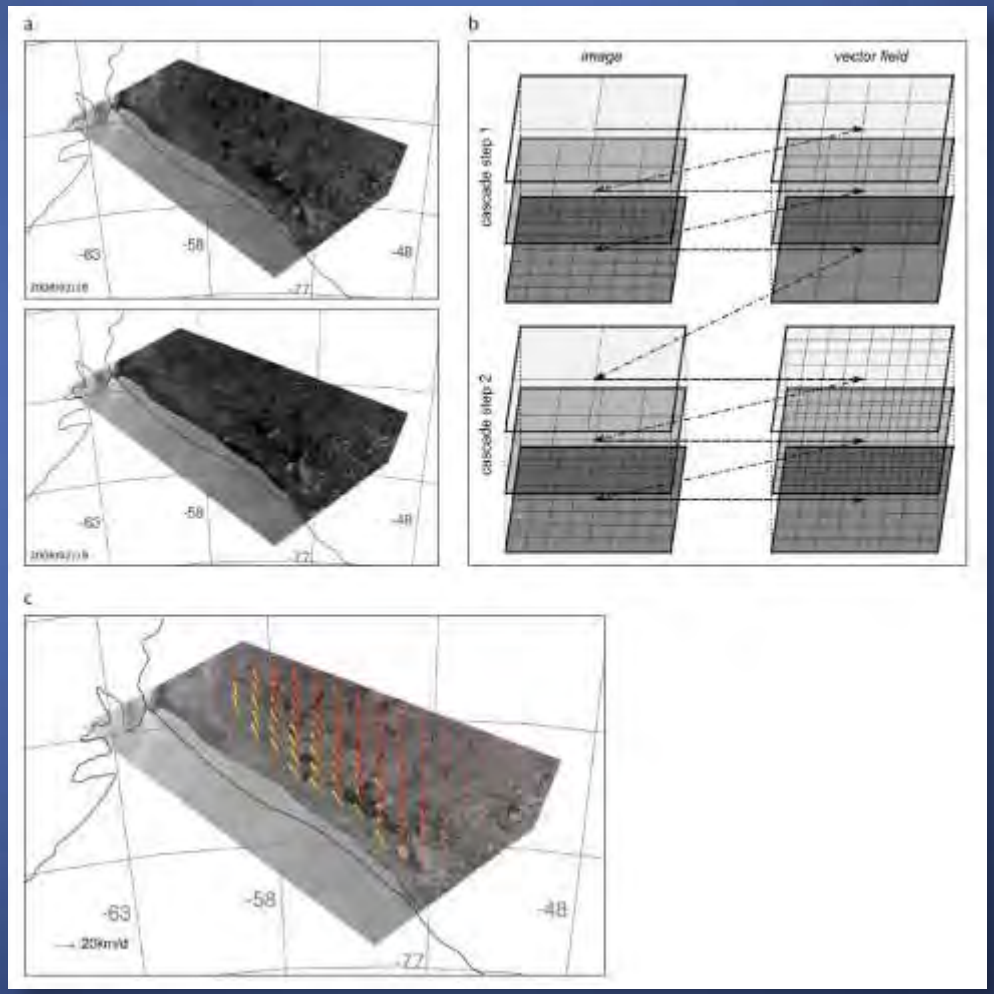

Drift analysis: resolution pyramids linked in a cascade

[Dierking 2013]

Sea Ice
Take-Home Messages

Ice detection (icebergs)
Classification through multi-pol SAR
Ice drift

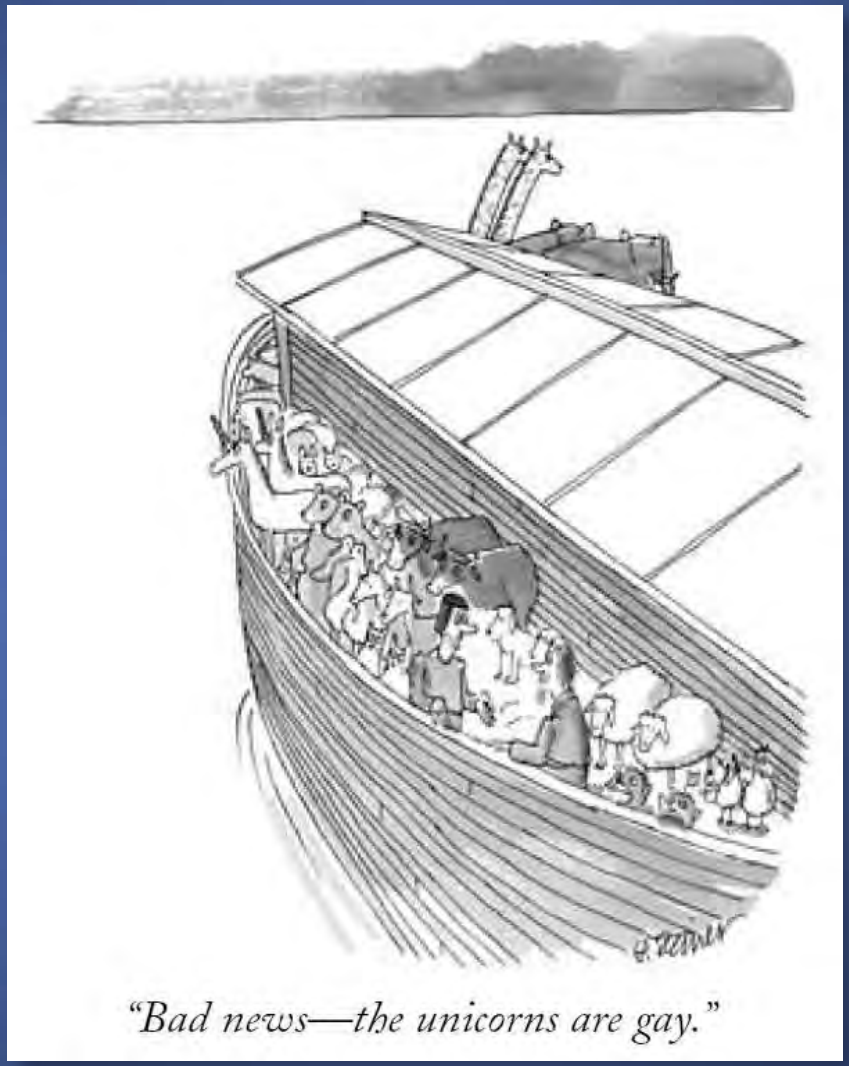

"Bad news—the unicorns are gay."

it's time for practicals…